



Initial Diagnosis and Staging of Pancreatic Cancer Including Main Differentials

Axel Dallongeville, MD, Lucie Corno, MD, Stéphane Silvera, MD, Isabelle Boulay-Coletta, MD, and Marc Zins, MD

Computed tomography (CT) remains the optimal imaging modality for both diagnosis and staging of pancreatic adenocarcinoma. Especially, CT is highly accurate in assessing the relationship of the tumor to critical arterial and venous structures, since their involvement can preclude surgical resection or indicate a neoadjuvant strategy in borderline resectable or locally advanced lesions. MRI provides additional staging information in isodense tumors or regarding presence of small liver metastases not seen at CT. Endoscopic ultrasound is the reference technique to be used for obtaining histologic proof. The introduction of perfusion modalities and radiomics may benefit the evaluation of pancreatic lesion parameters, thus helping to rule out differentials. However, these techniques require further investigation and standardization.

Semin Ultrasound CT MRI 40:436-468 © 2019 Elsevier Inc. All rights reserved.

Introduction

Pancreatic cancer is the fourth most common source of cancer mortality and the second cause of death from malignancies involving the digestive system (after colorectal cancer).¹ Furthermore, the current sharp rise in the incidence of pancreatic cancer may make the disease the second leading cause of cancer death by 2030, before colorectal cancer.² The many diagnostic and therapeutic advances achieved in recent decades have not reversed the extremely grim prognosis, and fewer than 5% of patients survive beyond 5 years.^{3,4} Contributors to the high mortality rate include the usually late diagnosis, early metastatic dissemination, and often limited response to chemotherapy and radiotherapy.⁵ Only complete excision with tumor-free (R0) margins can provide a cure.⁶ Imaging, by establishing the diagnosis, classifying the tumor, and determining the tumor stage plays a decisive role in determining whether the best treatment option is primary surgery or – as is increasingly the case – neoadjuvant chemotherapy or radiotherapy. In some cases, the imaging findings indicate that only palliative treatment is in order.

Risk Factors

Mean age at diagnosis is 70 years. Pancreatic cancer is more common in industrialized countries and in males.

The main risk factors are smoking, type 2 diabetes, chronic pancreatitis, obesity, and an inactive lifestyle. Genetic factors associated with pancreatic cancer include the *PRSS1* and *SPINK1* mutations responsible for hereditary pancreatitis, Peutz-Jeghers syndrome, and the *BRCA1* and *BRCA2* mutations that cause familial breast and ovarian cancer.⁷

Clinical Presentation

As most patients have no early symptoms and the late symptoms are variable and nonspecific, the disease is often advanced at first presentation. The type and timing of the symptoms depend chiefly on the location of the primary and on the stage of the tumor. Compared to location in the tail of the pancreas (20%-30% of cases), location in the head (70%-80% of cases) results in earlier symptoms including jaundice due to compression of the main bile duct. The most common symptoms are fatigue, anorexia, and weight loss, which are often delayed. Severe abdominal pain radiating toward the back suggests an unresectable tumor that has spread to the peritoneum.⁸

About 50% of patients with pancreatic cancer have diabetes mellitus.⁹ The diabetes may be a recent consequence of pancreatic duct obstruction by the tumor with pancreatic

Radiology Department, Groupe Hospitalier Paris Saint Joseph, Paris, France. Address reprint requests to Marc Zins, MD, Radiology Department, Groupe Hospitalier Paris Saint Joseph, Paris, France. E-mail: Mzins@hpsj.fr

tissue atrophy upstream of the blockage or of a paraneoplastic syndrome. Some patients, in contrast, have longstanding uncontrolled diabetes.

Acute pancreatitis due to obstruction of the main pancreatic duct may be the inaugural manifestation. The tumor may be challenging to diagnose as it may be masked by the pancreatic infiltration due to the acute disease.

Laboratory Findings

CA 19.9 is the main serum marker for pancreatic cancer. Sensitivity is 80% and specificity in symptomatic patients is about 80%-90%. The positive predictive value is too low, however, for diagnostic or screening purposes.¹⁰ Furthermore, false-positive results are common, notably in patients with cholestasis, diabetes, chronic pancreatitis, or other malignancies. Thus, CA 19.9 assay results must be interpreted with discernment.

The CA 19.9 level may supply prognostic information in 2 situations. At the diagnosis of pancreatic cancer, a value below 200 U/mL suggests resectability and a value above 1000 U/mL strongly suggests metastatic dissemination. During treatment monitoring, reversion to negativity after surgery has favorable prognostic significance, and declining values during chemotherapy or radiation therapy suggest satisfactory tumor control.¹¹

TNM Classification

Pancreatic cancer is currently classified using the 8th version of the American Joint Committee on Cancer (AJCC) staging system (Tables 1 and 2), which introduced several changes in the T and N categories compared to the earlier versions.¹²

The T category describes the size of the primary tumor measured along its largest dimension, as opposed to spread beyond

the pancreas in the 7th version. The new version is more objective and produces a closer correlation with survival.¹³

The N category describes the regional lymph nodes, for which no consensual definition exists to date. Tumors of the head or isthmus classically drain to nodes located about the hepatic pedicle, common hepatic artery, portal vein, and pylorus; anterior or posterior to the pancreaticoduodenal vessels; along the superior mesenteric vein; and along the right lateral border of the superior mesenteric artery. Tumors in the body or tail of the pancreas are believed to connect to nodes along the common hepatic artery, celiac artery, splenic artery, and splenic hilum.

Involved nodes at other sites are classified as remote metastases (M).

Figure 1 illustrates the TNM classification.

Diagnostic Imaging Studies

Ultrasound

Indications

Ultrasonography is the first-line imaging study in patients with jaundice or abdominal pain. This noninvasive and inexpensive investigation¹⁴ can visualize bile or pancreatic duct obstruction, detect the tumor, and contribute to assess spread by showing local and regional involvement and by detecting remote metastases (eg, liver metastases and retroperitoneal nodes). Nonetheless, slice imaging must be performed to further assess tumor spread. Ultrasonography can be used to guide a percutaneous biopsy (eg, of a liver metastasis or, more rarely, of the primary tumor).

Results

Published data on diagnostic performance vary considerably, in part due to the heavily operator-dependent nature of

Table 1 TNM (Tumor/Nodes/Metastasis) Classification for Pancreatic Cancer, Based on the American Joint Committee on Cancer (AJCC), 8th Edition (2010)

Stage	Definition
Primary Tumor (T)	
T1	Maximum tumor diameter ≤ 2 cm T1a: Maximum tumor diameter ≤ 0.5 cm T1b : Maximum tumor diameter >0.5 cm and ≤ 1 cm T1c: Maximum tumor diameter >1 cm and ≤ 2 cm
T2	Maximum tumor diameter $>2, \leq 4$ cm
T3	Maximum tumor diameter >4 cm
T4	Tumor involves the celiac axis, common hepatic artery or the superior mesenteric artery
Regional lymph nodes (N)	
N0	No regional lymph node metastasis
N1	Metastasis in 1–3 regional lymph nodes
N2	Metastasis in ≥ 4 regional lymph nodes
Distant metastasis (M)	
M0	No distant metastasis
M1	Distant metastasis

Table 2 Stages of Pancreatic Cancer Based on the AJCC Classification

Staging	T	N	M
Stage IA	T1	N0	M0
Stage IB	T2	N0	M0
Stage IIA	T3	N0	M0
Stage IIB	T1-T3	N1	M0
Stage III	T4 (any T)	Any N (N2)	M0
Stage IV	Any T	Any N	M1

ultrasonography. Thus, sensitivity has ranged from 50% to 90%.¹⁵⁻¹⁷

The main limitations of ultrasonography are related to the following factors:

- Tumor size smaller than 2 cm or causing little compression of the bile ducts or main pancreatic duct;
- Tumor location in the left side of the pancreas, notably the tail, which is less easily accessible by ultrasound;
- Tumors that cause diffuse infiltration of all or part of the pancreas without changing the gland contours and/or tumors that are isoechoic to the rest of the gland; and
- The usual technical limitations such as obesity and bowel gas obscuring the pancreas.

Direct signs. Pancreatic adenocarcinoma is typically visible as a hypoechoic and ill-defined image (Fig. 2) that may or may not modify the contours of the gland.¹⁸

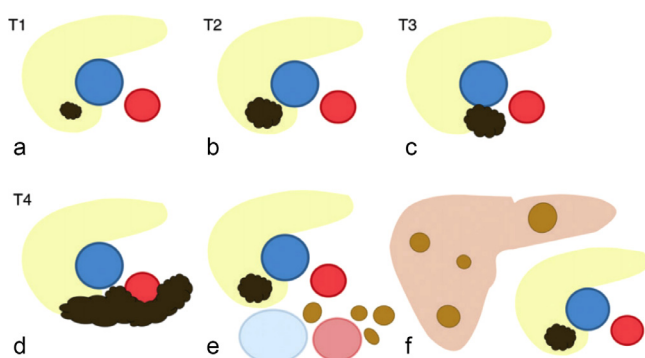


Figure 1 Staging of pancreatic adenocarcinoma. (a, b) Stage I is defined as a primary tumor confined to the pancreas (T1, <2 cm or T2, >2 cm) without nodal involvement or metastatic disease. (c) Stage IIA is disease extending beyond the pancreas without vascular involvement (T3), nodal involvement, or metastatic disease. (d) Stage IIB is defined as a primary tumor that has spread to the lymph nodes. (e) Stage III is disease that has spread to the blood vessels (T4). (f) Stage IV is disease with distant metastases. Blue, superior mesenteric vein; red, superior mesenteric artery; brown, primary tumor; gold, involved nodes and liver metastases; light blue, inferior vena cava; pink, aorta.²⁴ (Color version of figure is available online.)

Indirect signs. The many indirect signs include the following:

- Dilation of the main bile duct and intrahepatic bile ducts (if the tumor is in the head of the pancreas);
- Evidence of obstructive chronic pancreatitis upstream of the tumor such as dilation of the main pancreatic duct (>3 mm) and atrophy of the pancreatic parenchyma; and
- A pseudocyst due to acute pancreatitis upstream of the tumor.

Contribution of contrast-enhanced ultrasound (CEUS). Contrast-enhanced ultrasound (CEUS) was first evaluated in the late 1990s. The injection of a contrast agent that remains within the vascular network provides information on tissue blood supply. In several studies, CEUS performed better than conventional ultrasound and, in some cases, as well as computed tomography (CT).^{17,18}

Pancreatic adenocarcinoma is typically hypovascular, whereas chronic pancreatitis produces moderate and continuous enhancement with similar vascularity to that of the adjacent parenchyma; however, in very longstanding cases

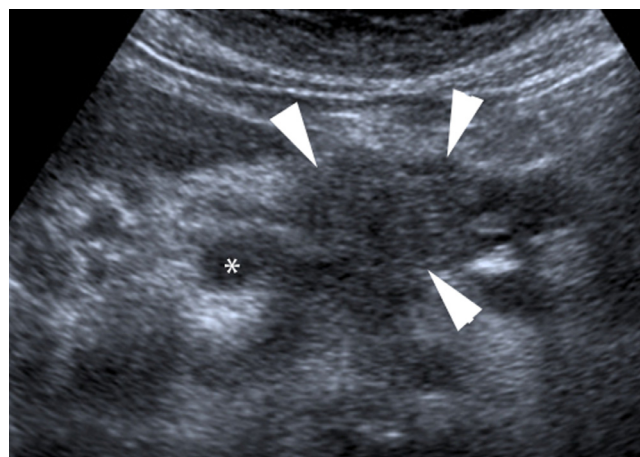


Figure 2 Ultrasound findings in pancreatic cancer. Transcutaneous abdominal ultrasound scan, transverse slice: Hypoechoic image in the pancreatic head (white arrowheads) and upstream dilation of the main pancreatic duct (asterisk).

with marked fibrosis, chronic pancreatitis may appear hypovascular. Although diagnostic performance was satisfactory in several studies,¹⁹⁻²¹ CEUS is heavily operator-dependent and rarely used in clinical practice.

Contribution of transcutaneous ultrasound elastography (TUE).

TUE is used routinely for some organs such as the breast and thyroid and was evaluated recently for the evaluation of pancreatic lesions. For the pancreas, however, TUE seems more challenging and less reproducible, due to the deep location of the gland and to the presence of artifacts related to bowel gas and aortic pulsations. TUE may help to distinguish pancreatic adenocarcinoma, which has a lower elasticity coefficient (blue image), from chronic pancreatitis (green image). Sensitivity is low, however, as some areas of pancreatitis with severe fibrosis may have a low elasticity coefficient.^{22,23} Although TUE might help to detect early pancreatic lesions, further studies, and better standardization are needed, and at present this technique is very rarely used in everyday practice.

Computed Tomography

Indications

CT is probably the most widely used imaging modality for pancreatic abnormalities. The goals are to establish the diagnosis and to assess locoregional and metastatic spread. CT is the only imaging technique that is indicated, in addition to ultrasound, in patients with metastatic pancreatic cancer.²⁴

Recommended Protocol for Pancreatic CT²⁵⁻²⁷

Helical multidetector CT is used to obtain multiphase acquisitions with a slice thickness of less than 3 mm. Multiplanar reconstruction is then performed to optimize the evaluation of tumor spread to the blood vessels, notably the veins.²⁸ An iodinated contrast agent is injected intravenously, in a concentration of at least 300 mg/mL, a volume of 1.5 mL/kg, and a high rate of 3 to 5 mL/s in most cases. The following acquisitions are obtained:

- An unenhanced acquisition;
- A delayed arterial or pancreatic acquisition, about 35-50 seconds after the beginning of the injection; reducing the field of view is optional but improves spatial resolution; and
- A portal phase acquisition, 70 seconds after the beginning of the injection.

Opacification of the upper gastrointestinal tract by having the patient ingest about 500 mL of water over the 10 minutes preceding the investigation helps to identify gastric and duodenal landmarks.

After image transfer to a postprocessing console, 2D and 3D reconstructions are generated. The peripancreatic blood vessels are evaluated on thick-slab maximum intensity projection (MIP) reconstructions.

Unenhanced acquisition: Investigation of the entire supracolic abdominal cavity

The goals are to:

- a) Detect any pancreatic calcifications;
- b) Look for spontaneous high attenuation, which might indicate bleeding; and
- c) Determine the exact height of the pancreas to optimize the pancreatic acquisition and decrease the radiation dose.

A low-dose protocol should be used.

Delayed arterial or pancreatic acquisition: the images are centered on the pancreas, extending from just above the origin of the celiac artery to the level of the third part of the duodenum.

The goal is to obtain a detailed evaluation of the pancreas and surrounding region and to examine the blood vessels, notably the arteries. Diagnostic performance is best at the pancreatic phase due to the greater density gradient between the tumor and normal pancreas compared to the pure arterial and parenchymal phases.^{26,29} This acquisition also allows the identification of anatomical variants of the arteries that may be of therapeutic significance (eg, presence of a right hepatic artery).

Portal phase acquisition: investigation of the entire abdomen and pelvis

This acquisition visualizes the veins and detects any hepatic and peritoneal metastases. As part of the staging workup, images can also be acquired at the thorax to look for lung metastases.

Results

As with ultrasound, the CT diagnosis of pancreatic adenocarcinoma relies on both direct and indirect signs.

Direct signs. Pancreatic adenocarcinoma is typically visible as an ill-defined area of hypoattenuation at the pancreatic phase and of either hypo- or isoattenuation at the portal phase (Fig. 3). This pattern is seen in 90% of cases. The remaining 10% are isoattenuating lesions (see challenging situations below). A large tumor may alter the contours of the gland.

Indirect signs (Fig. 4). The indirect signs may occur in isolation. They vary with the location of the tumor.

– Bile duct dilation upstream of the tumor

This sign is present in about 86% of patients with involvement of the pancreatic head.³⁰ The intrahepatic bile ducts are often dilated also, and the gallbladder may be distended (gall bladder hydrops).

– Main pancreatic duct dilation upstream of the tumor

The frequency of this sign is 88% for tumors of the pancreatic head and nearly 50% for those of the pancreatic body.³⁰ The secondary ducts may or may not be dilated also.

The double-duct sign, defined as dilation of both the bile duct and the main pancreatic duct, is highly suggestive of pancreatic cancer even when no other abnormalities are visible. The duct cutoff indicates the level of obstruction by the

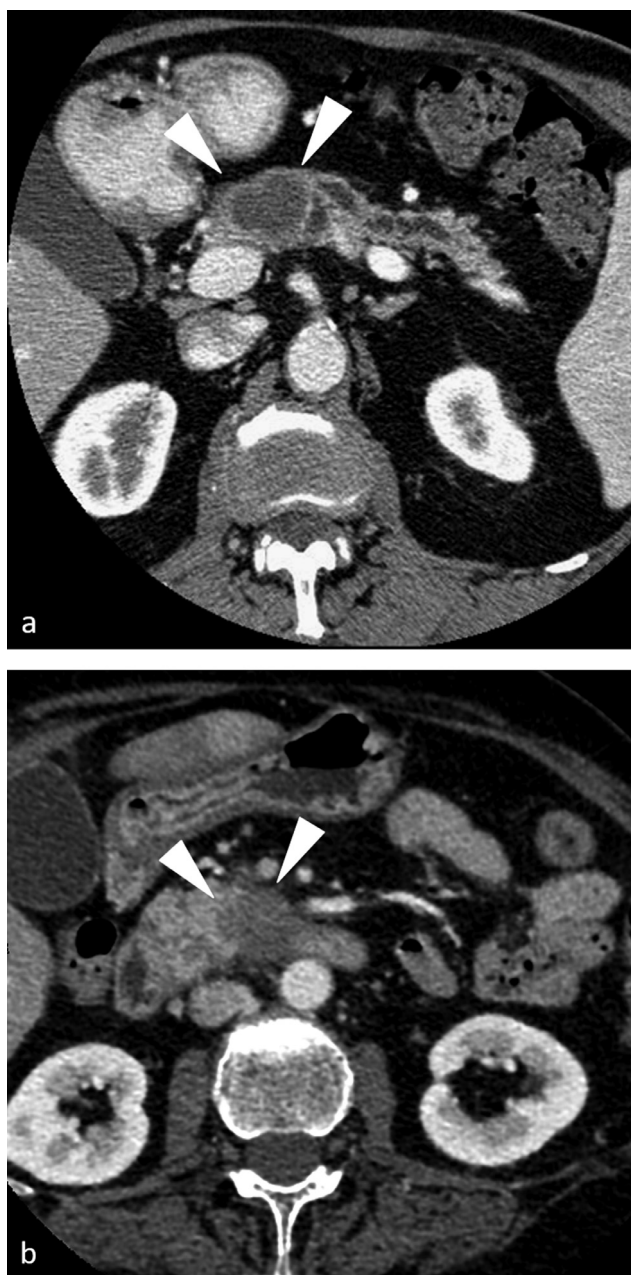


Figure 3 Direct signs of pancreatic cancer by computed tomography (CT). Contrast-enhanced CT, arterial pancreatic phase, axial views showing. (a) An ill-defined hypoattenuating image in the pancreatic isthmus (white arrowheads) with upstream parenchymal atrophy and main pancreatic duct dilation and (b) An ill-defined hypoattenuating image in the uncinate process (white arrows).

tumor, even when this last is isoattenuating and therefore not visible directly.

– Parenchymal atrophy upstream of the tumor

Parenchymal atrophy is a consequence of pancreatic duct obstruction and indicates postobstructive pancreatitis. This mechanism explains why the main pancreatic duct is often

dilated (about 82% of cases). Partial parenchymal atrophy with a normal-sized or enlarged downstream gland contrasting with atrophy of the upstream parenchyma strongly suggests cancer, even when the tumor is not directly visible.

– Pseudocyst upstream of the tumor

One or more pseudocysts may develop upstream of the tumor as a result of either acute pancreatitis or rupture of a dilated secondary pancreatic duct. This sign is seen in only about 8% to 10% of cases. The pseudocyst may obscure the primary tumor and therefore mistakenly suggest a cystic tumor or acute pancreatitis due to another cause.

The diagnostic performance of CT for detecting pancreatic adenocarcinoma is very good, with 89% to 97% sensitivity.³¹⁻³³ Performance is better for large tumors and decreases significantly, to only 67%-77%, for tumors measuring less than 20 mm.^{34,35}

Contribution of Spectral Imaging

New techniques have been developed to improve diagnostic performance, notably by increasing the contrast between the tumor and adjacent pancreas. One method consists in making the acquisitions at a lower energy of 80 kVp instead of the standard 120 kVp.³⁶ The more recent dual-energy spectral CT technique produces images at different energy levels and allows postprocessing to generate material-specific images, as well as monochromatic images. At low viewing energies, this technique may improve tumor detection.^{37,38} Virtual single-energy 70 keV images may provide the best compromise for evaluating tumor spread, notably to the blood vessels.³⁹

Challenging Situations

Isoattenuating tumors. Pancreatic adenocarcinoma exhibiting the same attenuation as the normal parenchyma on the arterial pancreatic and venous parenchymal acquisitions (Fig. 5) accounts for only 5.4% to 11% of all cases.^{40,41} Isoattenuation may correlate with small tumor size⁴² and has been reported in 27% to 40% of tumors smaller than 20 mm.^{33,43} The presence of indirect signs, notably involving the ducts, should suggest obstruction by a tumor and lead to further investigation by magnetic resonance imaging (MRI). MRI is nearly 80% sensitive for detecting isoattenuating pancreatic cancer.⁴⁴

Diffuse tumors. Diffuse involvement of the gland (Fig. 6) may occur in 5% to 20% of cases of pancreatic cancer.^{30,44} The absence of direct signs may raise diagnostic challenges: the pancreas is globally enlarged but there is no measurable mass or normal parenchyma to serve as a reference. In addition, when the left side of the pancreas is affected, the indirect signs of duct dilation and parenchymal atrophy are lacking also. Generalized gland enlargement, with a smooth appearance due to loss of the normal lobulations may be the only anomaly. Spread to nearby vessels seen, for instance, as splenic vein thrombosis or evidence of segmental portal

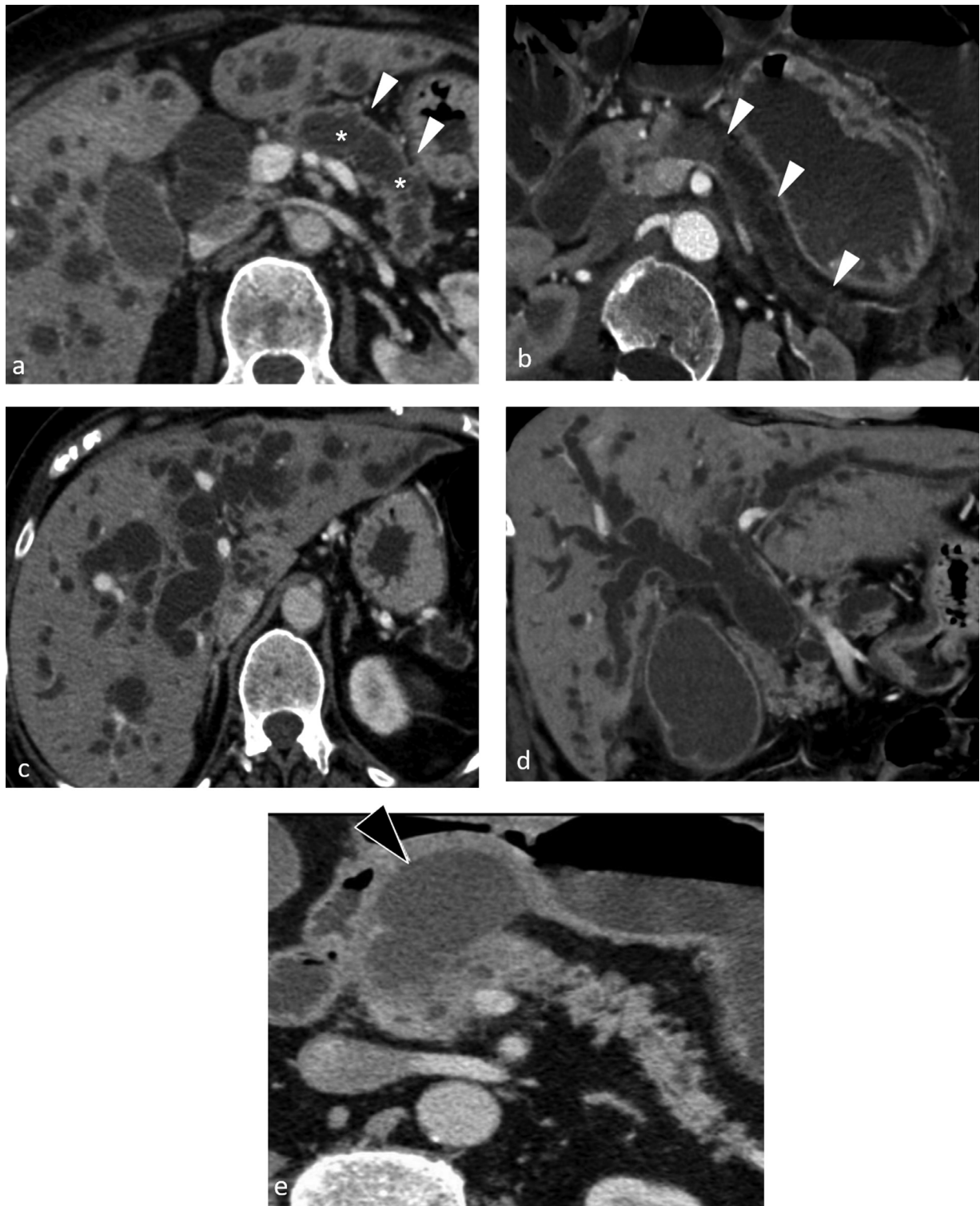


Figure 4 Indirect computed tomography (CT) signs of pancreatic cancer. Contrast-enhanced CT, axial views (a, b, c, and e) and coronal reconstruction (d). (a and b) Dilation of the main pancreatic duct (asterisk) and parenchymal atrophy (white arrowheads) upstream of a lesion in the pancreatic isthmus. (c and d) Dilation of the intra- and extrahepatic bile ducts upstream of a lesion in the pancreatic head. (e) Pseudocyst (black arrowhead) caused by fluid retention upstream of a lesion in the pancreatic head.

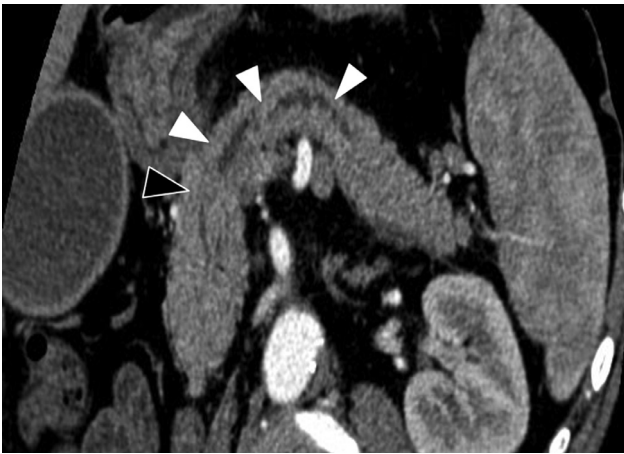


Figure 5 Isoattenuating pancreatic lesion by computed tomography (CT). Contrast-enhanced CT, arterial pancreatic phase, coronal reconstruction in the plane of the pancreatic duct showing dilation of the main pancreatic duct (white arrowheads) with a cutoff in the cephalic region (black arrowhead) and no visible parenchymal mass. Histology confirmed the diagnosis of pancreatic adenocarcinoma.

hypertension strongly suggests pancreatic cancer. The main differential diagnosis is autoimmune pancreatitis (AIP), which often produces generalized gland enlargement with failure to visualize the main pancreatic duct by CT. MRI is useful in this situation to differentiate a malignancy from autoimmune lesions.

Cystic forms of pancreatic adenocarcinoma. Cystic forms of pancreatic adenocarcinoma (Fig. 7) are extremely uncommon. The tumor is usually large, with a central area of necrosis. The cyst wall is often thick and uneven, and indirect signs are generally visible upstream of the lesion. The differential diagnoses are other cystic malignancies (eg, cystadenocarcinoma, mucinous cystadenoma or transformed intraductal papillary mucinous neoplasm, and solid pseudopapillary tumor).

Acute pancreatitis as the inaugural manifestation. Acute pancreatitis develops in about 10% of patients with pancreatic adenocarcinoma and may reveal the disease. As stated above, the underlying tumor may be hidden by the signs of acute pancreatitis: edema of the gland, peripancreatic fat stranding,

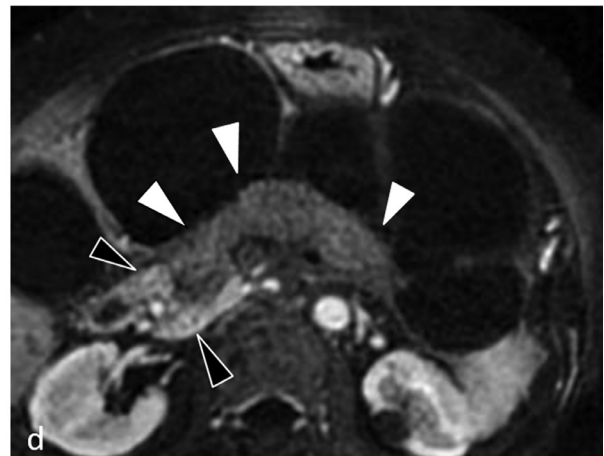
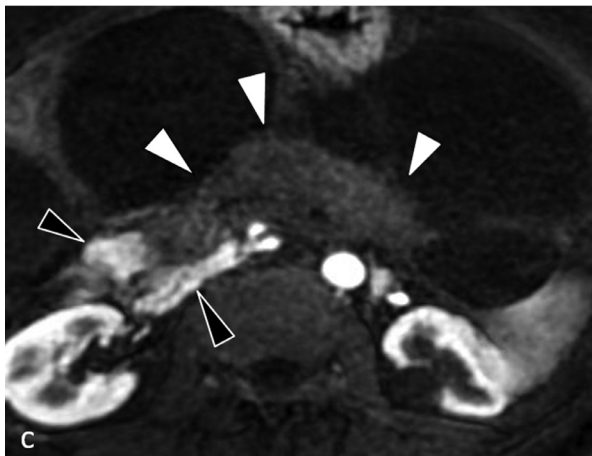
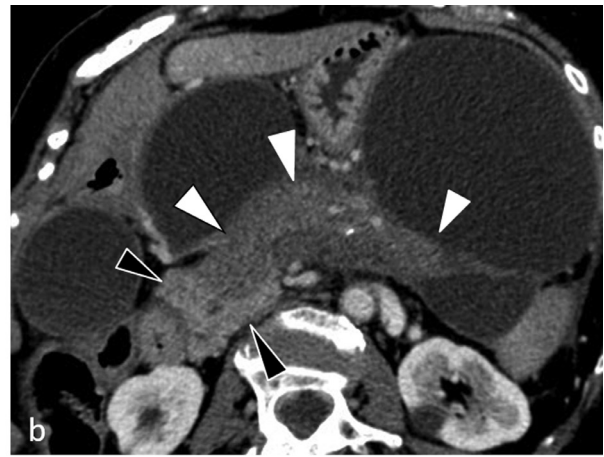


Figure 6 Computed tomography (CT) and magnetic resonance imaging (MRI) appearance of diffuse pancreatic adenocarcinoma. (a and b) Contrast-enhanced CT, axial views, (a) arterial pancreatic phase and (b) portal phase. (c and d) MRI, axial views, postgadolinium T1-weighted fat-suppressed GRE sequence at the arterial pancreatic phase (c) and portal phase (d). Note the diffuse involvement of the pancreatic body and tail (white arrowheads) that is hypoattenuating by CT and low signal by MRI compared to the normal cephalic parenchyma (black arrowheads).



Figure 7 Cystic form of pancreatic adenocarcinoma. Contrast-enhanced computed tomography, arterial pancreatic phase, axial view: Lesion in the pancreatic isthmus (black arrowhead) producing a hypoattenuating cyst-like appearance with upstream main pancreatic duct dilation and parenchymal atrophy.

and peripancreatic fluid collections (Fig. 8), hindering the diagnosis. In addition, several of the indirect signs of cancer (eg, main pancreatic duct dilation, pseudocyst, and vessel thrombosis) may occur also in pancreatitis.

In patients with acute pancreatitis, several findings should suggest pancreatic cancer, including location in the left side of the pancreas, evidence of obstructive pancreatitis (partial gland atrophy and segmental duct dilation), and sheathing of the blood vessels (notably the celiac artery or superior mesenteric artery).

When the diagnosis is in doubt, MRI should be performed to guard against missing a tumor.

Magnetic Resonance Imaging

Indications

Excellent contrast resolution is among the main advantages of MRI. Another is the ability to obtain not only a conventional structural assessment but also images of the ducts, by magnetic resonance cholangiopancreatography (MRCP), which is a noninvasive alternative to endoscopic retrograde cholangiopancreatography (ERCP). In addition, the introduction of diffusion imaging has improved the detection of primary tumors and, to an even greater extent, of hepatic and peritoneal metastases.

Although no universal recommendations are available, the use of MRI is advocated in at least the following two situations:

- Presence by CT of an isoattenuating tumor, as MRI usually provides better direct visualization of the lesion⁴⁵; and

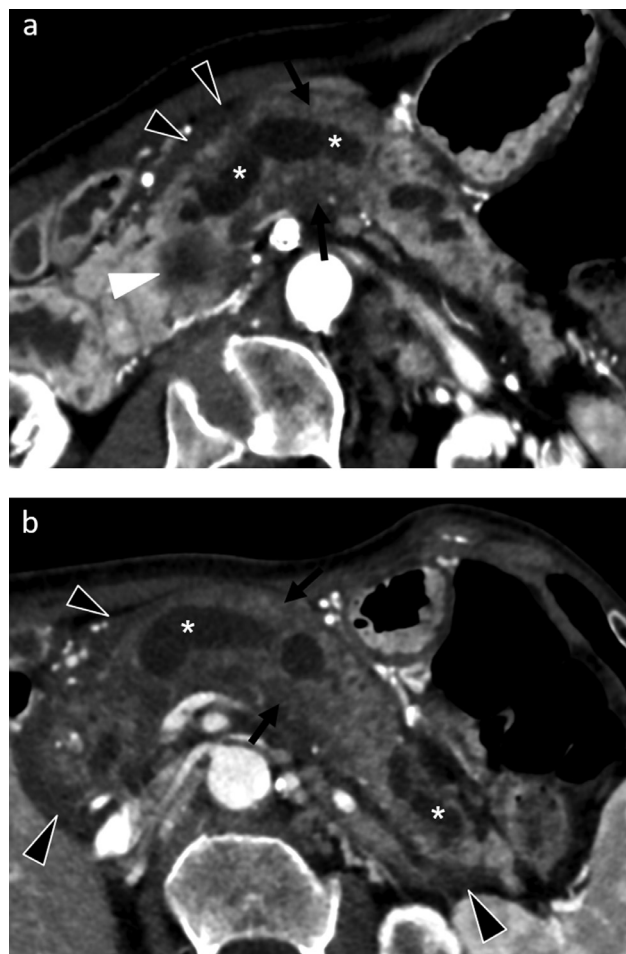


Figure 8 Pancreatic adenocarcinoma revealed by an episode of acute pancreatitis. Contrast-enhanced computed tomography, arterial pancreatic phase, axial views (a and b): Lesion in the pancreatic head (white arrowhead) with upstream main pancreatic duct dilation (asterisks) and signs of acute pancreatitis consisting of hypoattenuating parenchymal edema (black arrows) and infiltration of the peripancreatic fat (black arrow heads).

- Presence of a nonmetastatic tumor at CT, chiefly to detect hepatic metastases missed by CT (false-negative CT findings).

Technique

Although variations exist across centers, the MRI protocol used for the pancreas must include both structural sequences before and after gadolinium chelate injection and 2D or 3D MRCP sequences. The patient should be in the fasting state and medicated with a spasmolytic agent to limit motion artifacts produced by peristalsis.

We believe the protocol below provides an optimal assessment of pancreatic cancer.

Before gadolinium chelate injection

- T2-weighted single-shot fast spin-echo (SSFSE): Coronal and axial planes, section thickness <6 mm;

- T2-weighted fat-suppressed fast spin-echo (FSE): Axial plane, section thickness <6 mm;
- T1-weighted fat-suppressed spoiled gradient-echo with weighted in-phase and opposed-phase gradient echo (GRE): Axial plane, section thickness <6 mm;
- Diffusion-weighted imaging (DWI) with a large field of view including the liver: Axial plane, section thickness <6 mm;
- Preintravenous and dynamic postintravenous contrast 3D T1-weighted fat-suppressed GRE (arterial, portal venous, and equilibrium phases); and
- T2-weighted MRCP, 2D and/or 3D fast recovery FSE: Coronal and oblique planes, section thickness <3 mm for 3D and <20 mm for 2D.

This protocol is summarized in Table 3.

Results

Direct signs (Fig. 9). Direct tumor visualization is usually better by MRI than by CT. As a rule, the tumor generates low signal on T1-weighted fat-suppressed unenhanced images. On T2-weighted images, tumor visibility is often limited, with only a faint and heterogeneous high signal. On 3D T1-weighted images after gadolinium chelate injection, the tumor is hypointense compared to the adjacent pancreas at the arterial phase, which provides the best contrast between the enhanced normal pancreatic parenchyma and the less enhanced fibrotic tumor. Enhancement increases gradually. At the portal and late phases, the tumor is frequently isointense and therefore undetectable. However, the presence of a fibrotic component within the tumor may result in slight hyperintensity at the late phase.⁴⁶

Contribution of diffusion-weighted imaging (DWI)

The introduction of DWI has improved both the detection and the characterization of pancreatic tumors. DWI should therefore be used routinely.

DWI has excellent diagnostic performance for pancreatic lesions, with 96% sensitivity and 98.6% specificity.⁴⁷ Nevertheless, a study by Fukukura et al demonstrated that DWI was not the best sequence for accurately measuring and delineating the tumor,⁴⁸ chiefly due to marked hyperintensity of the adjacent pancreatic parenchyma.

The high cell density and presence of a fibrotic component usually result in restricted diffusion within pancreatic adenocarcinomas, whose apparent diffusion coefficient (ADC) is

therefore lower than that of benign lesions.⁴⁹ Although ADC cutoffs have been suggested, considerable overlap occurs, as ADC values vary with the degree of tumor differentiation and amount of fibrosis.⁴⁹ In addition, the lack of standardization of DWI protocols is a major obstacle to comparisons of published studies. In a recent meta-analysis, the mean ADC of pancreatic lesions was $1.332 \cdot 10^{-3} \text{ mm}^2/\text{s}$, with standard deviations of 0.78 to 2.32.⁵⁰

ADC may correlate with tumor aggressiveness, thus providing prognostic information. Low ADC values may be associated with a higher risk of spread to the blood vessels and peripancreatic nerve plexuses,⁵¹ a high risk of remote metastases, and worse survival.⁵² High ADC values, in contrast, may predict resectability with tumor-free resection margins (RO) in patients with borderline-resectable tumors.⁵³ High b-values must be used. A b-value of 1500 s/mm² with 3.0-T DWI may increase the sensitivity of tumor detection.⁵⁴ DWI and ADC mapping can detect nodules within cyst walls, thus indicating the presence of malignant transformation.

The main limitation of DWI is that malignancies cannot be distinguished from mass-forming chronic pancreatitis (MFPC). In addition, whether DWI helps to characterize cystic pancreatic lesions remains unknown.

DWI may be extremely useful for detecting remote metastases, notably in the liver and peritoneum (see the section on staging below).

Indirect signs (Fig. 10). The indirect signs of pancreatic cancer by MRI are the same as by CT. Signs of upstream obstructive chronic pancreatitis are clearly visible on the T1-weighted fat-suppressed sequence without contrast injection and include parenchymal atrophy and loss of the normal T1 high signal upstream of the tumor, whereas downstream size and signal are normal. MRCP shows irregular dilation of the main pancreatic duct, combined with dilation or visibility of the secondary ducts upstream of the tumor. MRCP also provides an accurate evaluation of the duct cutoff zone at the junction of the slender downstream duct and dilated upstream duct.

Endoscopic Ultrasound (EUS)

Indications

The main benefit derived from upper gastrointestinal tract EUS is the collection of specimens for cytological and/or

Table 3 Protocol for MRI Assessment of Pancreatic Adenocarcinoma

Sequence	Plane	Section Thickness
T2-weighted single-shot fast spin-echo (SSFSE)	Coronal and axial	< 6 mm
T2-weighted fat-suppressed fast spin-echo (FSE)	Axial	< 6 mm
T1 weighted fat-suppressed spoiled gradient-echo and with weighted in-phase and opposed-phase gradient echo GRE	Axial	< 6 mm
Diffusion-weighted imaging	Axial	< 6 mm
Pre-and dynamic post-intravenous contrast 3D T1-weighted fat-suppressed GRE (arterial, portalvenous and equilibrium phases)	Axial and Coronal	As thin as possible (<3mm)
T2-weighted MRCP : 2D and/or 3D FR FSE	Coronal and oblique	20 mm for 2D < 3 mm for 3D

Note: MRCP, magnetic resonance cholangiopancreatography; 2D, two dimensional; 3D, three dimensional.

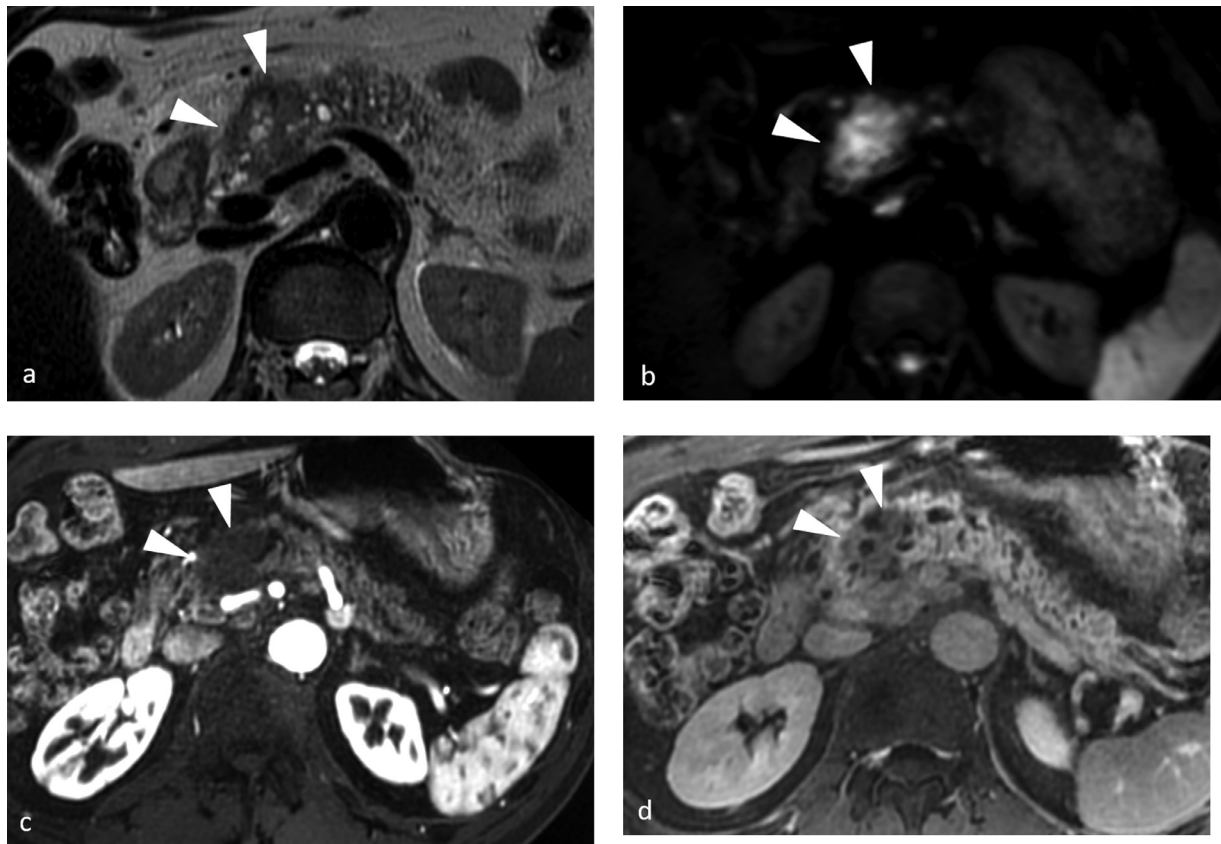


Figure 9 Direct signs of pancreatic adenocarcinoma by magnetic resonance imaging. (a) T2 SSFSE, axial views. (b) Diffusion-weighted imaging, b800, axial views. (c and d) Contrast-enhanced T1-weighted fat-suppressed GRE sequence, axial views, arterial pancreatic phase, (c) and late phase (d). Pancreatic lesion in the isthmus (white arrowhead), measuring 25 mm, generating high signal on T2 images, high diffusion signal, and lower signal than the adjacent pancreatic parenchyma at the arterial pancreatic phase with gradual heterogeneous enhancement indicating the presence of a fibrous component.

histological studies. EUS may also provide information on locoregional spread that complements those obtained by CT. Nonetheless, EUS is not the reference standard investigation for assessing vascular invasion.

Regarding pancreatic adenocarcinoma, EUS is chiefly useful in 3 situations:

- strong suspicion of a pancreatic tumor and indirect signs by CT and/or MRI (notably main pancreatic duct dilation) but no visible tumor;
- visualization of a pancreatic lesion of uncertain nature (notably doubt regarding the possibility of AIP or MFCP); and
- need for a histological diagnosis (when no more easily accessible lesions exist), for instance before starting induction or neoadjuvant chemotherapy.

New EUS methods such as elastography and injection of an US contrast agent are being evaluated but are not recommended at present.

Obtaining Histological Documentation by EUS

Histological documentation of nonmetastatic tumors is usually obtained by fine needle biopsy under EUS guidance. EUS biopsy performs similarly to percutaneous biopsy, with

88%-90% sensitivity and nearly 100% specificity, and has a lower complication rate of 1.38% compared to 5.6%.^{55,56} A 19G, 22G, or 25G needle is generally used. Unfortunately, histological proof may be challenging to obtain if the tumor is small, located deep in the gland or, most importantly, contains a predominant fibrous component with a marked desmoplastic reaction. As a result, the negative predictive value of fine needle biopsy is only about 55%-65%.⁵⁷ The presence of underlying chronic pancreatitis also adversely affects diagnostic performance, diminishing sensitivity to 55%-74%.⁵⁸

EUS-guided fine needle biopsy may be the histological sampling method of choice for resectable tumors in the right side of the pancreas, as the risk of dissemination may be lower with the transduodenal than with the percutaneous approach. Another major advantage is that the biopsy tract is removed in its entirety with the operative specimen if duodenopancreatectomy is performed.

The recognized indications of EUS-guided fine needle biopsy are as follows:

- Typical, potentially resectable tumor, being considered for neoadjuvant therapy;
- Unresectable tumor considered for chemotherapy, with no remote metastases that would be more readily accessible to percutaneous biopsy (eg, liver, peritoneum); and

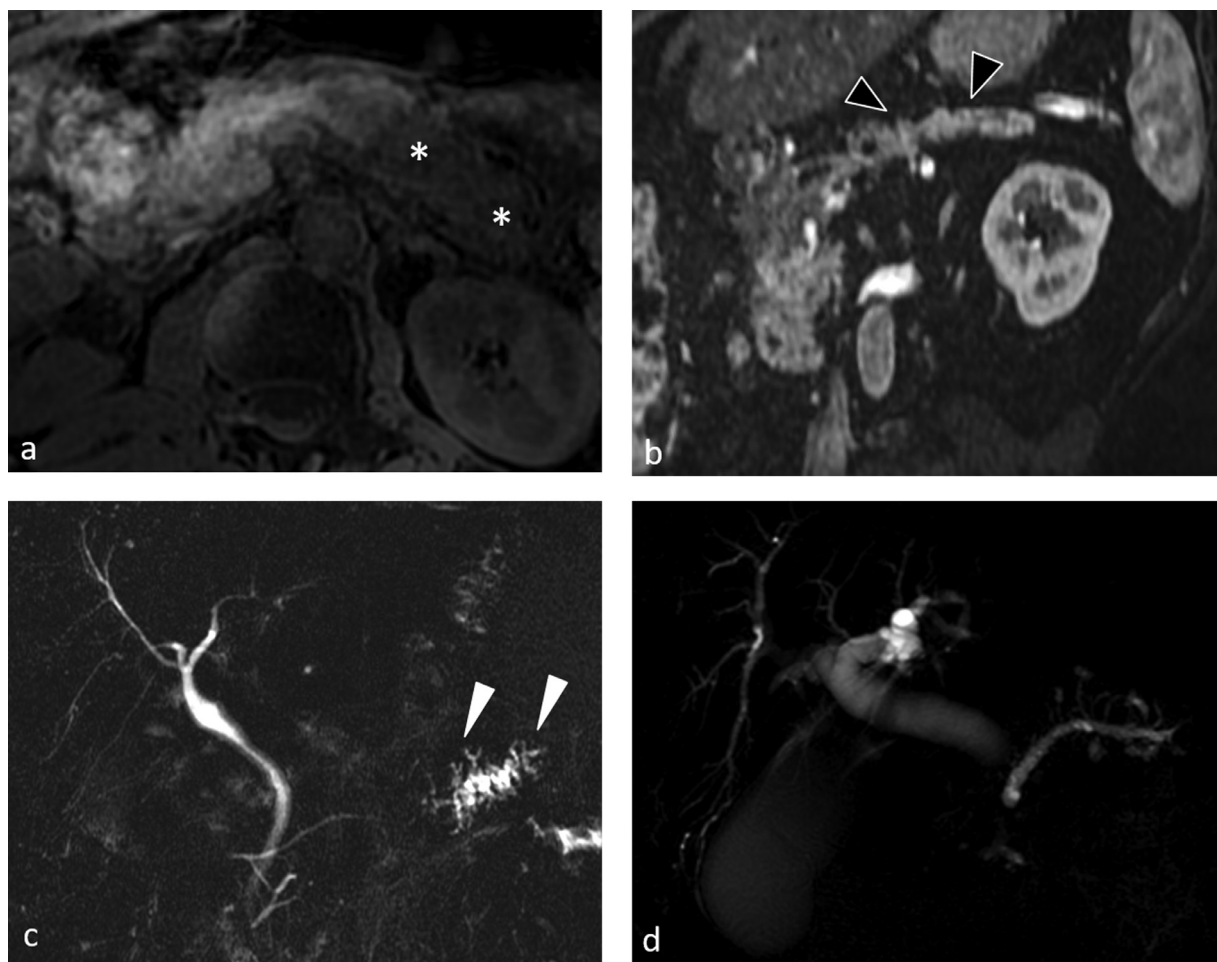


Figure 10 Indirect signs of pancreatic adenocarcinoma by magnetic resonance imaging. (a) Unenhanced T1-weighted fat-suppressed GRE sequence, axial view: loss of the normal parenchymal high signal on T1 images (asterisk) upstream of a lesion in the pancreatic isthmus. (b) Postgadolinium T1-weighted fat-suppressed GRE sequence, coronal view: Parenchymal atrophy (black arrowheads) upstream of a lesion in the isthmus. (c and d) T2-weighted magnetic resonance cholangiopancreatography sequences, 2D coronal view: (c) dilation of the main and secondary pancreatic ducts (white arrowheads) indicating chronic pancreatitis upstream of a lesion in the body and (d) dilation of the main pancreatic duct and intra- and extrahepatic bile ducts (double duct sign) upstream of a lesion in the pancreatic head for indirect signs.

- Diagnostic uncertainty with a need to rule out differentials (AIP, chronic pancreatitis, benign tumor).

In practice, however, EUS-guided fine needle biopsy is often performed routinely, although histological documentation is not mandatory when primary surgical resection is deemed feasible. Importantly, a negative biopsy in a patient whose imaging studies strongly suggest cancer should not delay the surgical treatment.

18-Fluorodeoxyglucose Positron Emission Tomography (FDG-PET) Combined With Computed Tomography (CT)

FDG-PET is not performed routinely in patients with pancreatic cancer, as it does not help to characterize the pancreatic lesions and does not perform better than CT or MRI for ruling out other diagnoses (notably chronic pancreatitis). In

addition, for the assessment of locoregional spread, FDG-PET performs less well than CT for visualizing the primary (particularly if <2 cm) and has only 37% sensitivity and 79% specificity for detecting positive regional nodes.⁵⁹

In contrast, FDG-PET is more effective than CT for detecting remote metastases, notably in the liver and peritoneum,⁶⁰ for which sensitivity is 88%-91% versus 30%-57% for CT. Nonetheless, MRI is superior over FDG-PET for detecting liver metastases, particularly those measuring less than 1 cm.

During the initial workup, FDG-PET should be used only when in doubt about the presence of remote metastases, notably involving the peritoneum or nodes (eg, in the retroperitoneal space).

FDG-PET Combined With MRI

FDG-PET combined with MRI is a recently introduced technique that may hold promise, as it provides both structural information via the MRI sequences (Fig. 11), notably DWI,

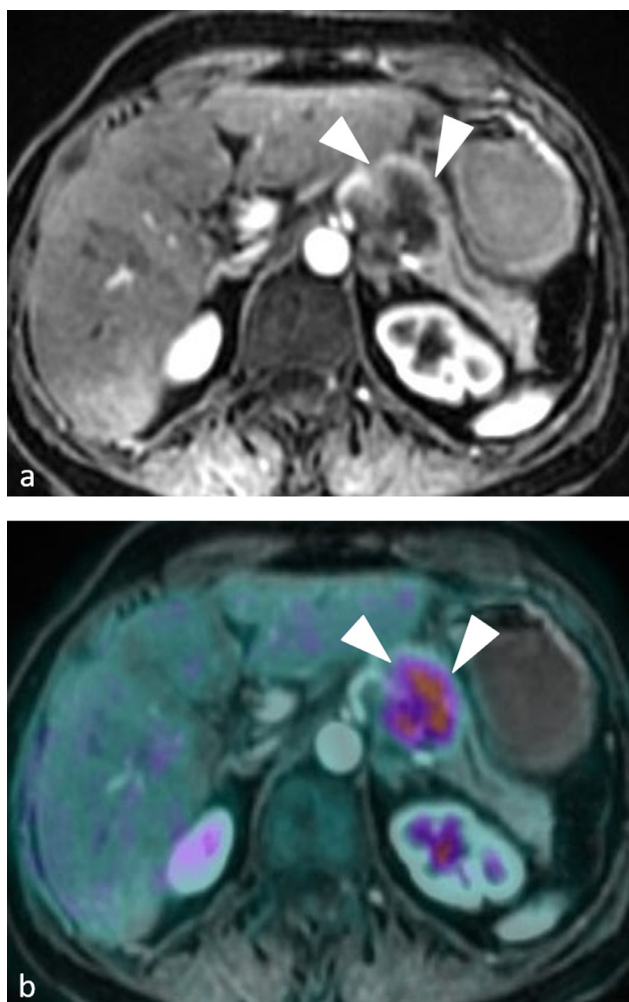


Figure 11 Appearance of pancreatic adenocarcinoma by 18-fluorodeoxyglucose positron emission tomography (FDG-PET) coupled with magnetic resonance imaging (MRI). (a) MRI, postgadolinium T1-weighted fat-suppressed GRE sequence, axial view at the arterial pancreatic phase. (b) Same view merged with the metabolic images obtained by FDG-PET. High uptake by a lesion in the body of the pancreas (white arrows) indicating a primary tumor. Courtesy of O. Lucidarme, Pitié, University Hospital, Paris, France. (Color version of figure is available online.)

and metabolic information. The contribution and indications of FDG-PET-MRI are under evaluation. A recent meta-analysis suggests that FDG-PET-MRI may have similar diagnostic performance to FDG-PET-CT plus contrast-enhanced multi-detector CT.⁶¹

Differential Diagnoses

Chronic Pancreatitis

Differentiating MFCP from pancreatic adenocarcinoma is the most difficult challenge raised by pancreatic imaging. In both conditions, the patient profile, clinical presentation (pain, weight loss, jaundice), and imaging findings, notably by CT, can be similar. In addition, the 2 conditions may co-exist (Fig. 12), as chronic pancreatitis is among the risk factors for

pancreatic cancer. In this situation, the diagnosis of cancer is often made late, at the stage of locally advanced or metastatic disease.

Pancreatic adenocarcinoma is highly fibrous and hypovascular, 2 characteristics shared by chronic pancreatitis. Consequently, a tumor that is well differentiated or contains an abundance of fibrous stroma may be difficult to diagnose on histological specimens. Similarly, MFCP may be seen by CT as a hypoattenuating mass that enhances gradually (indicating fibrosis) and is accompanied with indirect upstream signs (segmental atrophy and segmental duct dilation).

CT findings that suggest chronic pancreatitis rather than pancreatic cancer include intraductal or intraparenchymal calcifications, less pronounced and irregular upstream duct dilation, and a more gradual decrease in main bile duct diameter in contact with the lesion.

Triple-phase CT has been used to evaluate enhancement kinetics.⁶² Chronic pancreatitis produced a delayed washout pattern contrasting with gradually increasing enhancement of pancreatic adenocarcinoma. However, overlap occurred between the 2 patterns. In addition, this technique is ill-suited to clinical practice.

Recently developed functional imaging modalities seek to assist in differentiating chronic pancreatitis from pancreatic cancer.⁶³ Perfusion CT may provide diagnostic assistance but is not capable at present of definitively distinguishing between the 2 entities.⁶⁴ Finally, there is some evidence that absence of *KRAS* mutations (ie, presence of the wild-type gene) in pancreatic fluid strongly suggests a benign condition.⁵⁵

Contrast-Enhanced Ultrasound

Contrast agents specifically designed for ultrasonography can be used during standard transcutaneous ultrasound or EUS. Contrary to the contrast agents used for CT or MRI, they remain within the vascular network and consequently provide information on tissue blood supply.

Pancreatic adenocarcinoma is usually hypovascular. In contrast, moderate and continuous vascularization is seen in chronic pancreatitis, which appears isovascular to the adjacent normal parenchyma.⁶⁵ When used in combination with other ultrasound criteria, enhancement kinetics may improve the ability to distinguish among various pancreatic conditions.⁶⁶

However, longstanding MFCP may appear hypovascular.⁶⁷ In practice, CEUS is rarely used as it is both highly operator-dependent and unable to reliably differentiate benign and malignant lesions.

Perfusion CT

As discussed above, structural CT imaging may fail to distinguish pancreatic adenocarcinoma from MFCP, both of which may produce a hypovascular image at the pancreatic arterial phase, gradual enhancement, and indirect signs (postobstructive pancreatitis, notably with cephalic lesions). Analyzing the perfusion parameters may help to distinguish the vascularized tissue component from the fibrous component.

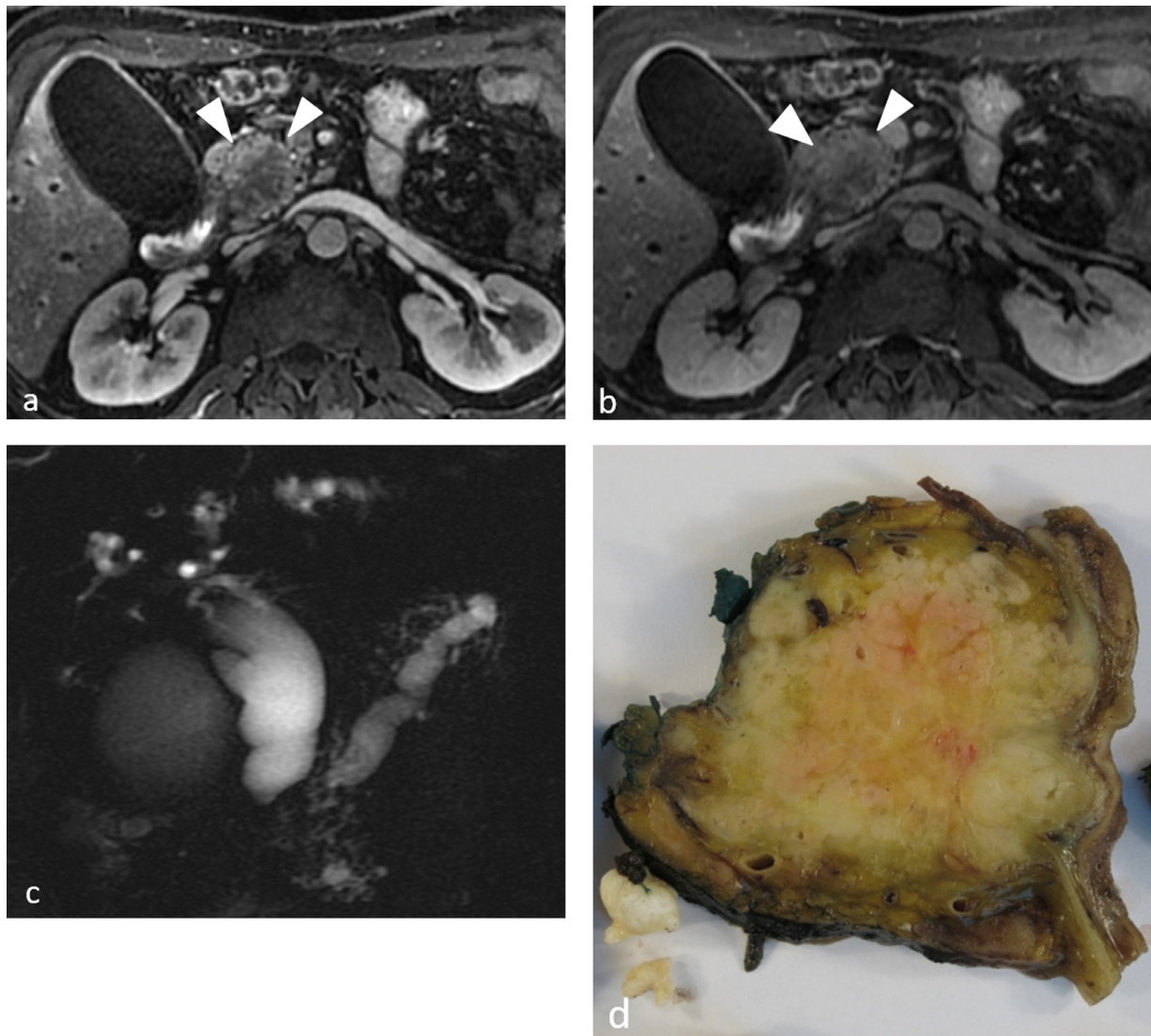


Figure 12 Pancreatic adenocarcinoma developing on calcified mass-forming chronic pancreatitis (MFCP) visualized by magnetic resonance imaging (MRI). (a and b) MRI postgadolinium T1-weighted fat-suppressed GRE sequence, axial views at the arterial pancreatic phase (a) and portal phase (b). (c) Magnetic resonance cholangiopancreatography, T2-weighted 2D sequence, coronal view. Lesion in the pancreatic head (white arrowheads) generating low signal compared to the adjacent parenchyma at the arterial phase, with gradual enhancement; Double duct sign on the Wirsung-MRI sequence. Several fine needle biopsies were negative. (d) Histological examination (only a, b and c actually) of the cephalic duodenopancreatic resection specimen showed an infiltrating adenocarcinoma. (Color version of figure is available online.)

With triple-phase pancreatic CT, enhancement kinetics falls into 3 patterns:

- Early washout pattern with an early peak at the pancreatic arterial phase followed by gradual washout of the normal parenchyma;
- Delayed washout pattern with a peak at 60-70 seconds followed by gradual washout of MFCP lesions; and
- Gradually increasing enhancement of pancreatic adenocarcinoma.

Comparing the enhancement value curves may perform well for distinguishing between MFCP and pancreatic adenocarcinoma, with 82%-94% sensitivity and 83%-90% specificity depending on the injection protocol.⁶² This tool may

therefore hold promise, although it appears ill-suited to clinical practice.

MRI, Diffusion, Perfusion

As indicated above, conventional acquisitions combining gadolinium-enhanced T2-weighted structural sequences with duct sequences have similar diagnostic performance to CT. Adding diffusion and perfusion sequences may help to differentiate pancreatic adenocarcinoma from MFCP.

Diffusion-weighted imaging (DWI)

Although DWI performs well for detecting pancreatic abnormalities (see the section on DWI-MRI), both pancreatic adenocarcinoma and MFCP are highly fibrous lesions that restrict diffusion, producing a high diffusion signal and a

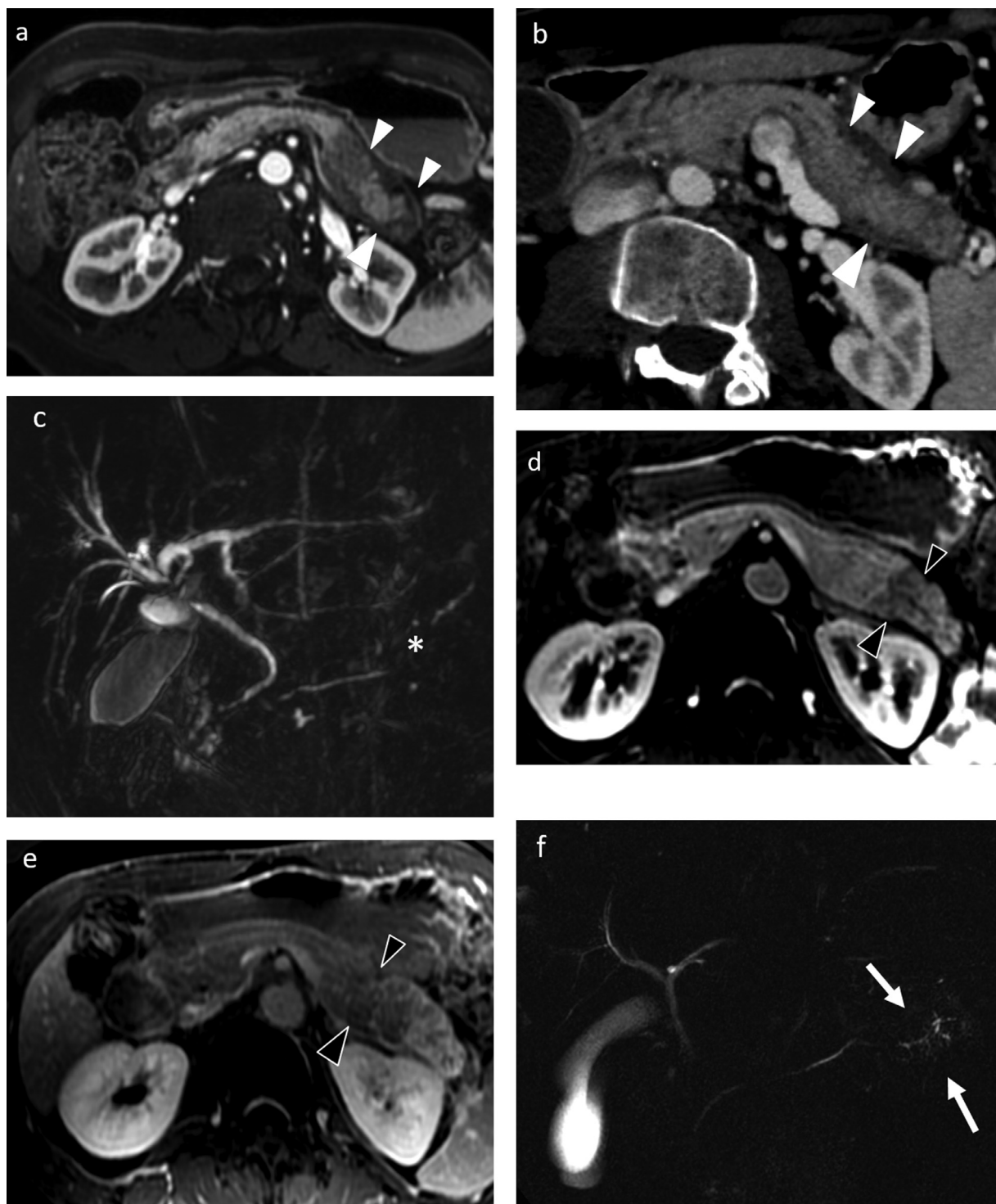


Figure 13 Examples of autoimmune pancreatitis by magnetic resonance imaging (MRI) and computed tomography (CT). (a, b, and c) Acute autoimmune pancreatitis of the tail: (a) MRI, postgadolinium T1-weighted fat-suppressed GRE sequence at the arterial pancreatic phase, axial view and (b) contrast-enhanced CT at the arterial pancreatic phase, axial view showing edema of the tail of the pancreas with a rim of low signal by MRI (halo sign) and of hypoattenuation by CT (white arrowheads); (c) magnetic resonance cholangiopancreatography, T2-weighted sequence, 2D coronal view: the main pancreatic duct is abnormally slender and is interrupted in several places in the caudal region (asterisk). (d, e, and f) Autoimmune pancreatitis of the body with upstream chronic pancreatitis by MRI: postgadolinium T1-weighted fat-suppressed GRE sequence, axial view, (d) arterial pancreatic phase and (e) late phase showing an ill-defined tumor-like image in the body of the pancreas (black arrowheads) with evidence of upstream parenchymal atrophy of the tail; (f) magnetic resonance cholangiopancreatography, T2-weighted sequence, 2D coronal view showing an abnormally slender main pancreatic duct in the body of the pancreas with no cutoff at the level of the tumor-like image, ruling out a primary tumor; note the dilation of the secondary ducts in the tail of the pancreas (white arrow) indicating upstream chronic pancreatitis.

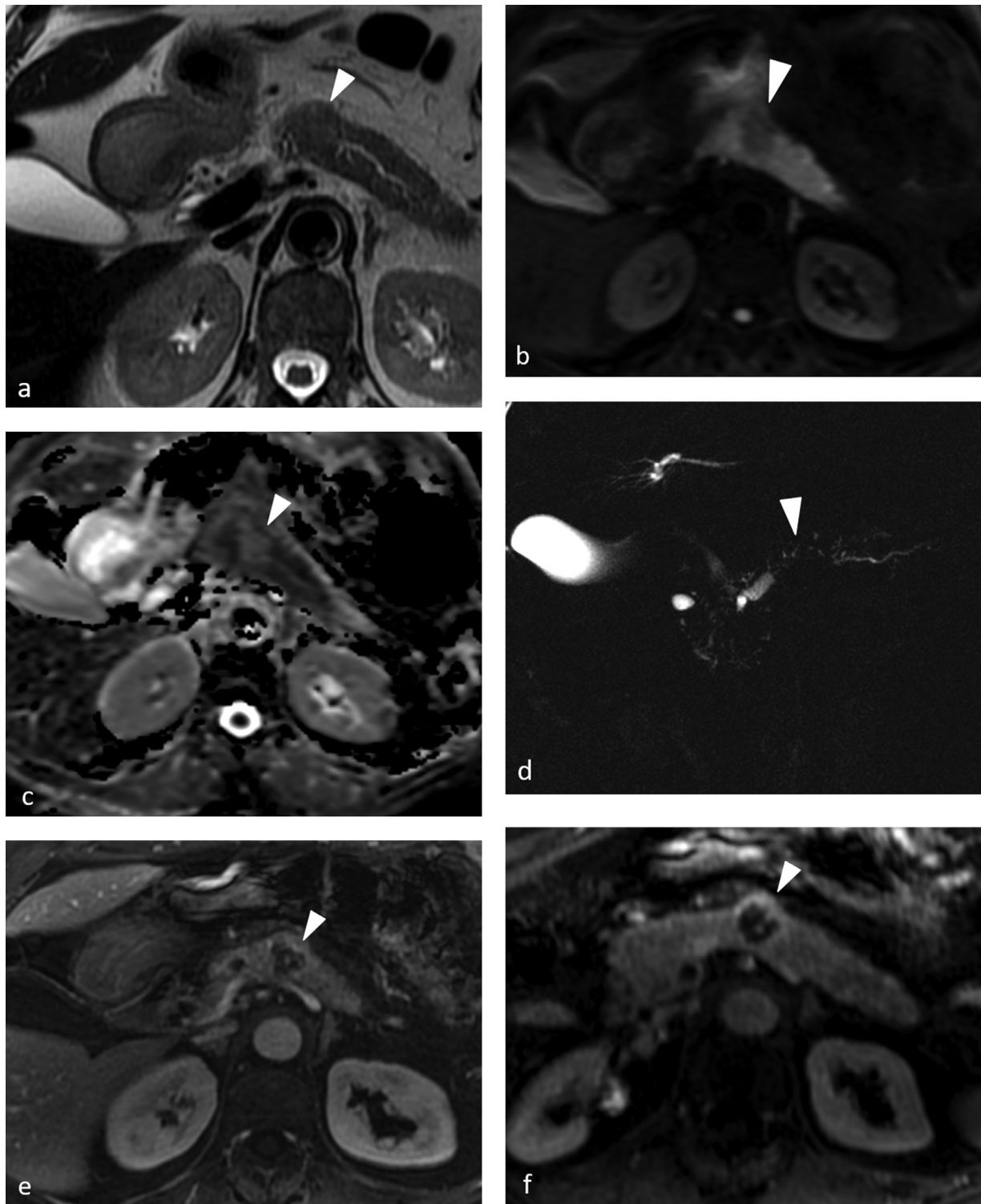


Figure 14 Autoimmune focal pancreatitis visualized by magnetic resonance imaging. (a) T2SSFSE sequence, axial views. (b) Diffusion-weighted imaging. (c) Apparent diffusion coefficient. (d) T2-weighted magnetic resonance cholangiopancreatography, 2D coronal view. (e) T1-weighted fat-suppressed GRE sequence at the portal phase, axial view. (f) 3D T1-weighted fat-suppressed GRE sequence at the portal phase. Lesion in the body of the pancreas generating intermediate signal on T2 images and low diffusion signal, with a high ADC value and gradual peripheral enhancement around a hypovascular center. Note the duct cutoff on the magnetic resonance cholangiopancreatography image with upstream signs of chronic pancreatitis. A biopsy collected by endoscopic ultrasound confirmed the diagnosis of autoimmune pancreatitis.

decrease in ADC values. ADC is significantly lower in pancreatic adenocarcinoma than in the normal parenchyma or MFCP.⁶⁸ Nonetheless, ADC values vary with tumor differentiation and the amount of fibrosis, so that considerable overlap exists between adenocarcinoma and MFCP. Thus, no reliable cutoffs exist for differentiating these 2 conditions.

Perfusion-weighted imaging (PWI)

As with CT, the perfusion parameters during MRI may help to distinguish pancreatic cancer from MFCP. However, research into PWI is still in its early stages and this method is therefore not suitable for clinical practice.

Autoimmune Pancreatitis (AIP)

AIP is a rare form of chronic pancreatitis that exists as 2 variants, Type 1 and Type 2,⁶⁹ whose main features are listed below.

- Type 1 (about 80% of all cases of AIP): Predominance in men, mean age at diagnosis of about 60-70 years, higher incidence in Asia, IgG4 elevation in many cases, and multiorgan involvement in some patients (eg, liver, kidneys, lungs)
- Type 2 (20%-30% of all cases of AIP): Affects males and females equally, younger mean age at diagnosis of about 40 years, usually normal IgG4 levels, and chronic inflammatory bowel disease in about 30% of cases

Imaging studies may show diffuse or focal involvement of the pancreas. Diffuse AIP is usually easy to distinguish from pancreatic cancer. Focal AIP predominantly involving the cephalic region may account for up to 67% of all cases of AIP⁷⁰ and can raise greater diagnostic challenges.

Clinical, laboratory, and imaging criteria have been suggested for the diagnosis of AIP, such as those developed by Hisort.⁷¹ IgG4 levels are elevated in about two-thirds of cases of type 1 AIP but are usually normal in type 2 AIP. The specificity of IgG4 elevation has been estimated at 95%.⁷² CA19-9 is often high in patients with cancer but is less helpful due to its low specificity, with other causes of elevation including AIP, as well as uncontrolled diabetes and cholestasis.

The main imaging study findings that suggest AIP are listed below.⁷³⁻⁷⁵

Pancreatic parenchyma

- Uniform enhancement of the mass at the portal and delayed phases
- Multiple pancreatic masses
- Hypointense capsule-like rim (halo sign)
- Absence of parenchymal atrophy upstream of the lesion
- Absence of spread to the adjacent blood vessels
- Marked restriction of diffusion <0.88

Abnormalities of the ducts

- Long stenoses of the main pancreatic duct (>3 cm) in a multifocal distribution, with little or no upstream narrowing
- Little or no dilation (<4 mm) of the main pancreatic duct upstream of the lesion
- Duct-penetrating sign, defined as penetration of the main pancreatic duct into the mass, with no stop sign
- Icicle sign, defined as a smooth tapered stenosis of the main pancreatic duct upstream of the mass.⁷⁶

MRI may perform better than CT for differentiating cancer from AIP. Reported sensitivities of these 2 investigations are

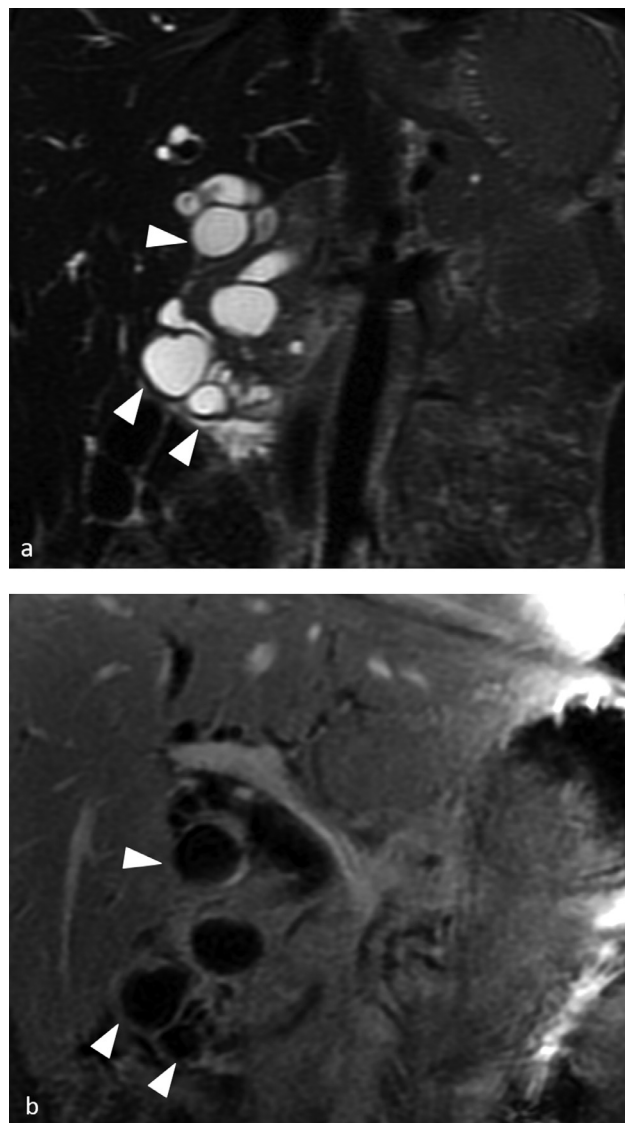


Figure 15 Paraduodenal pancreatitis by magnetic resonance imaging. (a) T2SSFSE sequence, coronal view. (b) Postgadolinium T1-weighted fat-suppressed GRE sequence at the portal phase, coronal view. Note the multiple cyst-like images in the paraduodenal region (white arrowheads indicating paraduodenal pancreatitis).



Figure 16 Pancreatic neuroendocrine tumor by computed tomography (CT) and magnetic resonance imaging (MRI). (a) Contrast-enhanced CT, arterial pancreatic phase. (b) MRI, postgadolinium T1-weighted fat-suppressed GRE sequence at the arterial pancreatic phase, axial view. Hypervascular, exophytic, partly calcified, 2-cm lesion in the tail of the pancreas (white arrowheads) with no dilation of the main pancreatic duct. The biopsy confirmed the diagnosis of well-differentiated neuroendocrine tumor. (c and d) Contrast-enhanced CT, arterial phase, axial views showing an ill-defined hypervascular mass in the pancreatic head (white arrow) and several hypervascular lesions in the liver. The diagnosis was pancreatic gastrinoma with liver metastases.

88.5%-90.2% vs 77%-80.3% for AIP and 97.5%-99.2% vs 91.8%-94.3% for cancer.⁷⁷

Autoimmune disease at another site (eg, cholangitis, renal involvement, or chronic inflammatory bowel disease) suggests AIP, whereas the presence of remote lesions indicates cancer.⁷⁸

Finally, the CT and MRI abnormalities usually resolve at least partially after a course of corticosteroid therapy, which serves as a diagnostic test. Consequently, when the diagnosis is in doubt, these investigations should be repeated after a short interval to avoid missing a malignant lesion (Figs. 13 and 14).

Paraduodenal Pancreatitis (PDP)

PDP is a focal form of chronic pancreatitis that involves the pancreaticoduodenal groove. This condition was formerly known as cystic dystrophy of heterotopic pancreas and is still sometimes designated groove pancreatitis. Middle-aged (about 40 years) males are predominantly affected, and about 80% of patients have chronic alcohol abuse.

PDP occurs as a cystic form and as a solid form that is more difficult to distinguish from pancreatic groove adenocarcinoma. PDP is also classified as either pure, ie, confined to the groove, with no spread to the parenchyma; or segmental, with involvement of both the groove and the adjacent parenchyma.⁷⁹

There are 3 main signs of PDP on imaging studies. Presence of all 3 signs should suggest the diagnosis.

- Focal mural thickening (>3 mm) of the second duodenum, more marked on the pancreatic side, with increased contrast enhancement
- Cystic formations in the duodenal wall or neighboring region (Fig. 15)
- Fibrous tissue filling the groove.

Some signs that may be present in PDP should nevertheless lead to a reappraisal of the diagnosis and suggest a malignancy if the groove is infiltrated. They include pancreatic

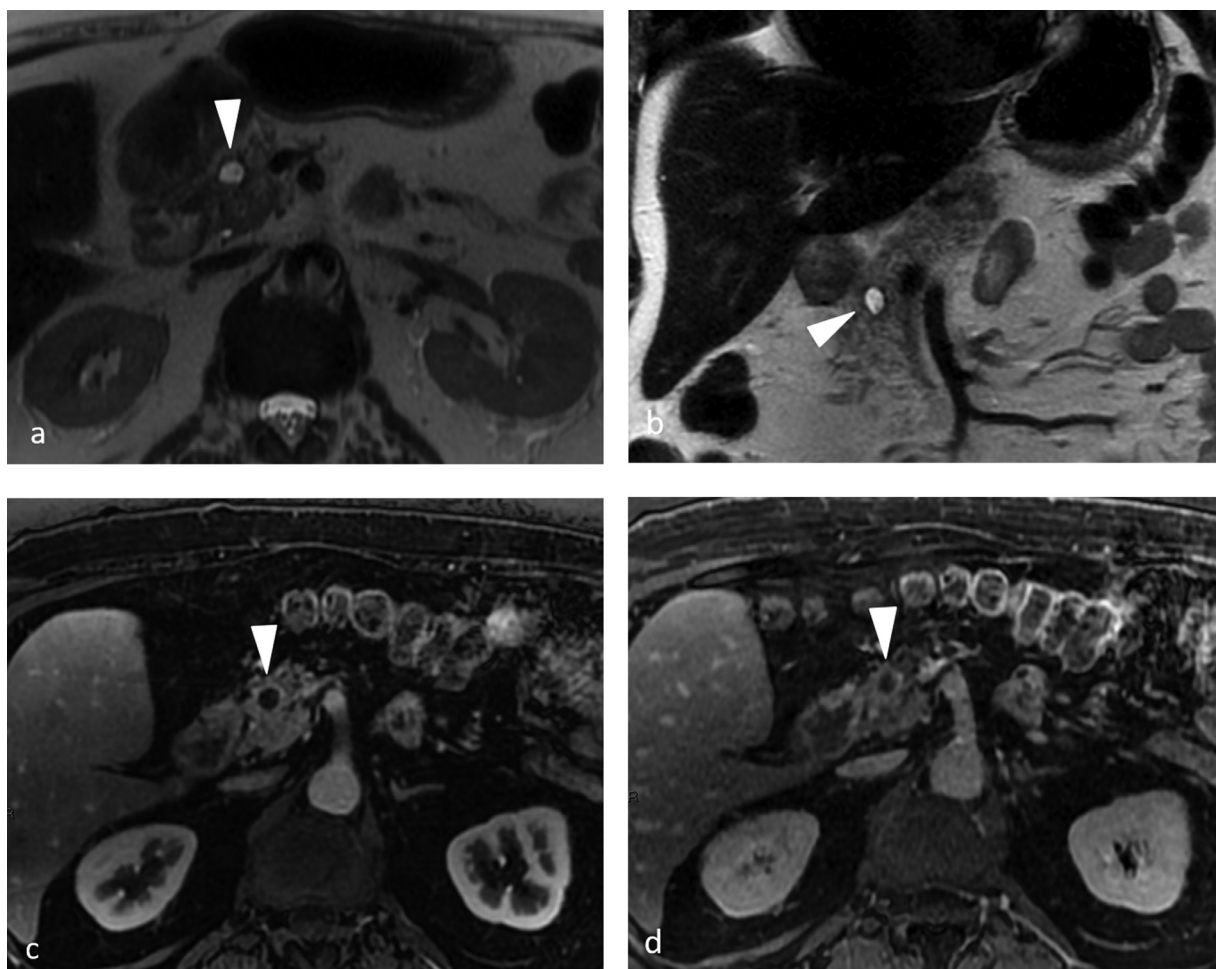


Figure 17 Cyst-like form of neuroendocrine tumor by magnetic resonance imaging (MRI). (a and b) T2SSFSE sequences, axial (a) and coronal (b) views. (c and d) Postgadolinium T1-weighted fat-suppressed GRE sequence at the (c) arterial pancreatic and (d) venous phases, axial views. Cyst-like, 11-mm lesion in the head of the pancreas (white arrowheads) generating high signal on T2 images, with a rim of contrast enhancement.

duct dilation, main bile duct dilation, encasement of the gastroduodenal artery, and invasion of the portal vein.

Neuroendocrine Tumors (NETs)

NETs account for only about 10% of all pancreatic tumors and are classified as functioning or nonfunctioning. High vascularity is a feature of the vast majority of NETs, notably those in the functioning category. As a result, NETs are usually readily differentiated from pancreatic adenocarcinoma. However, some NETs are not hypervascular and therefore raise diagnostic challenges.

Functioning NETs

Most functioning NETs cause symptoms and are therefore detected at an early stage. Imaging studies show a small, well-defined, solitary lesion that often has an abundant and uniform blood supply.

Nonfunctioning NETs

The diagnosis of nonfunctioning NETs is frequently established at a later stage, when the tumor is larger and has often

produced metastases, notably to the liver. Hypervascularity on imaging studies is less marked than with functioning NETs, and the differential diagnosis with pancreatic adenocarcinoma may therefore be more difficult. The tumor may have a heterogeneous appearance with necrotic foci, calcifications, or hemorrhagic remodeling.

In a patient with a pancreatic mass, imaging study findings that support a diagnosis of NET rather than of pancreatic adenocarcinoma include sharper mass contours, greater enhancement at the arterial pancreatic and portal phases (Fig. 16), and absence of upstream changes to the pancreatic ducts, bile ducts, or pancreatic parenchyma.⁸⁰ MRI usually shows high signal on T2-weighted images and high diffusion signal by DWI with an ADC value that is almost consistently lower than that of the adjacent parenchyma.⁸¹ The ADC value has been proven useful for detecting high-grade NETs. The optimal ADC cutoff was $1.19 \cdot 10^{-3} \text{ mm}^2/\text{s}$, with values below the cutoff having 100% sensitivity and 92% specificity for grade 3 NET.⁸²

Other presentations of NETs include cystic pattern with peripheral enhancement (Fig. 17) or purely cyst form without enhancement.⁸³

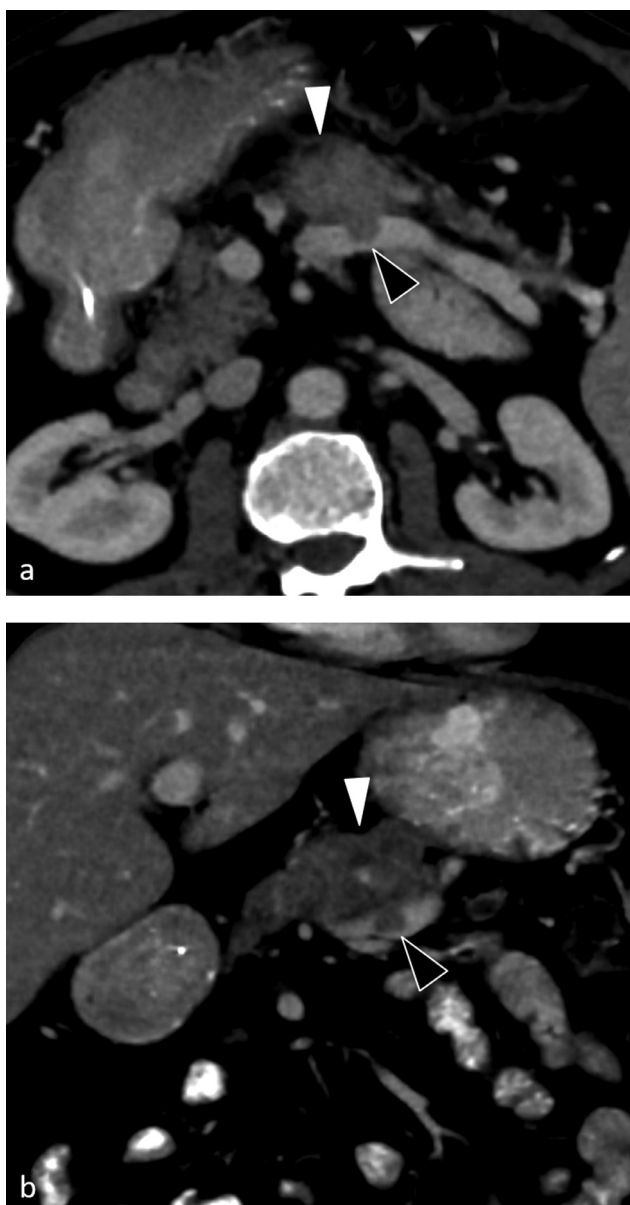


Figure 18 Neuroendocrine tumor with endovascular spread visualized by computed tomography (CT). (a and b) Contrast-enhanced CT, portal phase, (a) axial and (b) coronal views showing a tissular pancreatic lesion (white arrowheads) with endoluminal budding within the splenic vein (black arrowheads). This patient had a high-grade neuroendocrine tumor.

Spread to the veins often occurs as endoluminal invasion of a vessel located in contact with the tumor, in a pattern similar to that commonly seen in hepatocellular carcinoma (Fig. 18). In contrast, venous involvement with pancreatic adenocarcinoma generally occurs by direct spread, causing stenosis then occlusion of the vessel.

When the diagnosis is in doubt, isotopic investigations can be helpful. They include somatostatin receptor scintigraphy

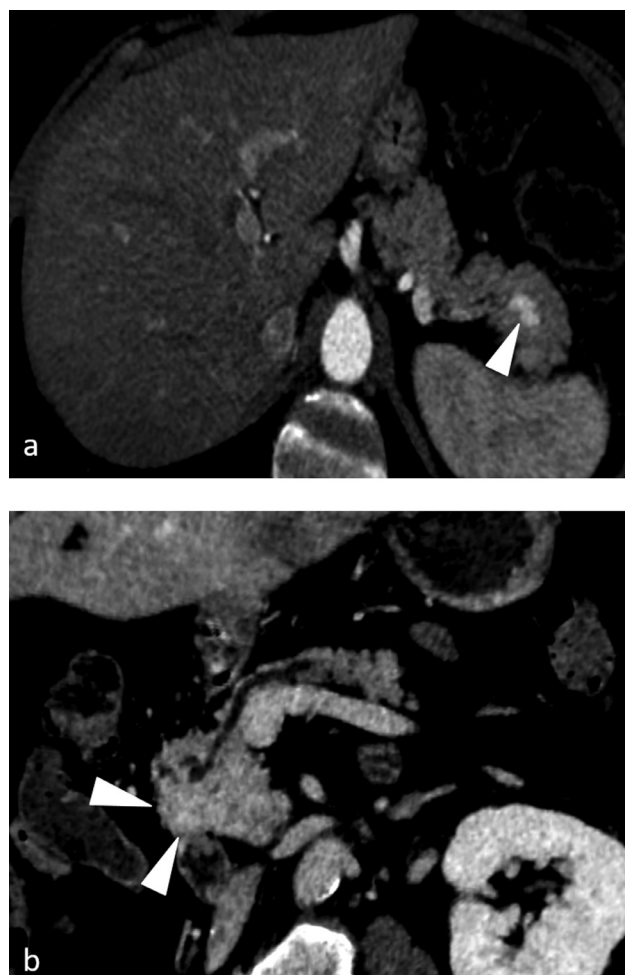


Figure 19 Two examples of renal carcinoma metastases to the pancreas by computed tomography (CT). Contrast-enhanced CT at the arterial phase, (a) axial view show hypervascular lesion in the tail and (b) coronal view show a hypervascular lesion in the head of the pancreas. Histology showed that both lesions were renal carcinoma metastases.

to detect well differentiated NETs and FDG-PET-CT for undifferentiated grade 3 NETs.

Other Rare Pancreatic Tumors

Apart from NETs, several other histological types of pancreatic malignancies exist, although they are far less common than pancreatic adenocarcinoma.

Pancreatic Metastases

Metastases rarely develop in the pancreas. The most common primaries are melanoma and cancers of the kidney, lung, breast, colon, and rectum.⁸⁴ The peripheral pancreas is most commonly involved. Both unifocal and multifocal forms exist. Absence of main pancreatic duct dilation is suggestive. Pancreatic metastases often share

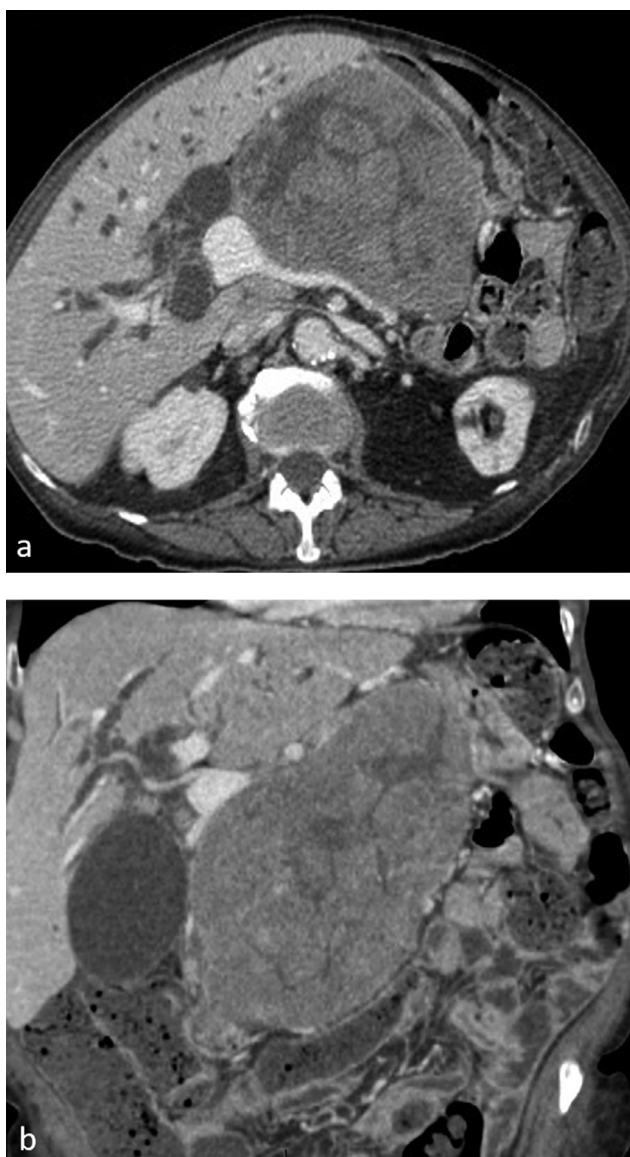


Figure 20 Acinar cell carcinoma by computed tomography (CT). Contrast-enhanced CT at the portal phase, (a) axial and (b) coronal views: large, sharply marginated, heterogeneous, oval lesion in the pancreas with exophytic development and a cyst-like component causing compression of the portal vein and dilation of the upstream bile ducts. Courtesy of M.P Vullierme, Beaujon University Hospital, Clichy, France.

the same enhancement characteristics as the primary. Most are hypoattenuating well-defined tumors, although metastases from renal cancer or melanoma may be hypervascular (Fig. 19) and must therefore be differentiated from NETs.^{85,86}

Acinar Cell Carcinoma

Acinar cell carcinoma contributes less than 1% of all pancreatic tumors. Imaging studies usually show a large, oval, sharply marginated mass, often with a capsule (Fig. 20). Enhancement after contrast injection is moderate and less marked than that of the adjacent parenchyma.⁸⁷ An

exophytic appearance is suggestive. Intraductal forms have been reported.⁸⁸

Challenges in the Management of Pancreatic Adenocarcinoma

Primary surgical resection followed by adjuvant chemotherapy is currently the reference standard treatment and can provide a cure in patients with pancreatic adenocarcinoma, provided tumor-free resection margins (R0) are achieved.⁵ Survival is lower and roughly similar to that seen with radiotherapy and chemotherapy alone when the margins contain microscopically visible tumor cells (R1) or macroscopically visible tumor tissue (R2).⁸⁹

The challenge therefore consists in identifying those patients in whom R0 resection is likely to be achieved. When surgery is not an option, chemotherapy is the main treatment. Resectability is assessed based on the vascular connections of the tumor and on the absence of remote metastases (see the section on staging below).

About 80% of patients are ineligible for surgery, either because of locally advanced disease precluding the achievement of R0 margins or because remote metastases have developed. Thus, only 20% of patients have potentially resectable disease.

Many studies conducted over the last few years suggest that neoadjuvant chemotherapy with or without radiotherapy may constitute an effective debulking strategy that decreases the tumor stage in about 30% of patients,⁹⁰ thereby converting locally advanced nonresectable tumors to resectable tumors with similar R0 resection rates and survival outcomes to those seen in patients with initially resectable tumors.⁸³ Based on these studies, a neoadjuvant treatment strategy has been developed for borderline-resectable or locally advanced pancreatic adenocarcinoma. This strategy has several advantages: observation during neoadjuvant therapy helps to identify patients who are not good candidates for surgery due to aggressive tumor behavior with early metastases (about 30%); if the tumor responds to neoadjuvant therapy, the likelihood of R0 resection increases; any micrometastases are rapidly sterilized; and the opportunity to assess tumor chemosensitivity, as well as patient tolerance to chemotherapeutic agents, helps to select patients to surgery.⁹¹ Neoadjuvant therapy is increasingly used but is not the reference standard and remains poorly standardized. Several randomized trials are currently evaluating the potential benefits.

Staging

Accurate staging is crucial in patients with pancreatic adenocarcinoma, as it governs the treatment decisions. Classifications developed to define resectability of pancreatic tumors include those from the National Comprehensive Cancer Network (NCCN), which was updated in 2018; the MD Anderson Cancer Center; and the American Society of Clinical Oncology (ASCO), published in 2017. The criteria used to define resectability differ across these 3 classification

Table 4 NCCN Criteria for Staging Pancreatic Adenocarcinoma

Vessels	Resectable	Borderline Resectable	Unresectable
SMV/PV	No contact, <180° without vein contour irregularity	>180° , <180° with deformity or vein thrombosis but allowing safe and complete resection and reconstruction, contact with IVC	Unreconstructible obstruction, contact with most proximal draining jejunal branch
CHA	No arterial tumor contact	Contact without extension to celiac axis or HA bifurcation	Contact with extension to CA or CHA bifurcation
CA	No arterial tumor contact	No contact (head), Contact < 180° (body and tail)	Contact >180° , any contact with aorta
SMA	No arterial tumor contact	Contact <180°	Contact >180° , contact with first jejunal SMA branch, contact with aorta

Note: CA, celiac artery; CHA, common hepatic artery; HA, hepatic artery; IVC, inferior vena cava; PV, portal vein; SMA, superior mesenteric artery; SMV, superior mesenteric vein.

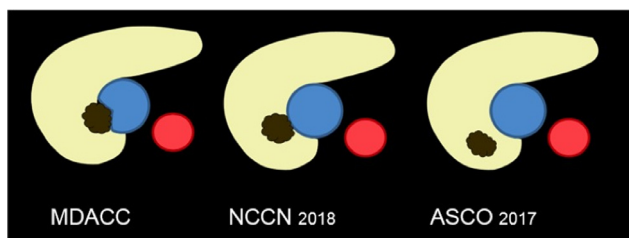


Figure 21 The 3 main classifications used to assess pancreatic tumor resectability. ASCO, American Society of Clinical Oncology; MDACC, MD Anderson Cancer Center; NCCN, National Comprehensive Cancer Network. (Color version of figure is available online.)

schemes. The NCCN classification defines resectability as absence of vascular spread or vein contact <180° without vessel lumen irregularity (Table 4). The ASCO classification uses a more restrictive definition requiring absence of CT evidence of vascular contact.⁹² MD Anderson Cancer Center criteria are less stringent, in contrast, as patent portal or mesenteric vein invasion does not rule out resectability.⁹³ Figure 21 illustrates the differences across these 3 classifications.

The NCCN classification is the most widely used at present and is therefore described in detail here. Tumors are divided into 3 categories: resectable, borderline-resectable, and nonresectable locally advanced or metastatic.⁸⁹

Resectable Tumors (Figs. 22 and 23)

- No arterial tumor contact (celiac axis [CA], superior mesenteric artery [SMA], or common hepatic artery [CHA])
- No tumor contact with the superior mesenteric vein (SMV) or portal vein (PV) or ≤180° contact without vein contour irregularity.

Borderline-Resectable Tumors (Fig. 24)

Arterial

Pancreatic head/uncinate process

- Solid tumor contact with CHA, without extension to CA or hepatic artery bifurcation, allowing for safe and complete resection and reconstruction
- Solid tumor contact with the SMA of ≤180°
- Solid tumor contact with variant arterial anatomy (eg, accessory right hepatic artery, replaced right hepatic artery, replaced CHA, and the origin of replaced or accessory artery); the presence and degree of tumor contact should be noted, if present, as it may affect surgical planning.

Pancreatic body/tail

- Solid tumor contact with the CA of ≤180°
- Solid tumor contact with the CA of >180° without involvement of the aorta and with intact and uninvolved gastroduodenal artery, thereby permitting a modified Appleby procedure (some panel members prefer this criterion to be in the unresectable category).

Venous

- Solid tumor contact with the SMV or PV of >180°, contact of ≤180° with contour irregularity of the vein or thrombosis of the vein but with suitable vessel proximal and distal to the site of involvement allowing for safe and complete resection and vein reconstruction.
- Solid tumor contact with the inferior vena cava (IVC).

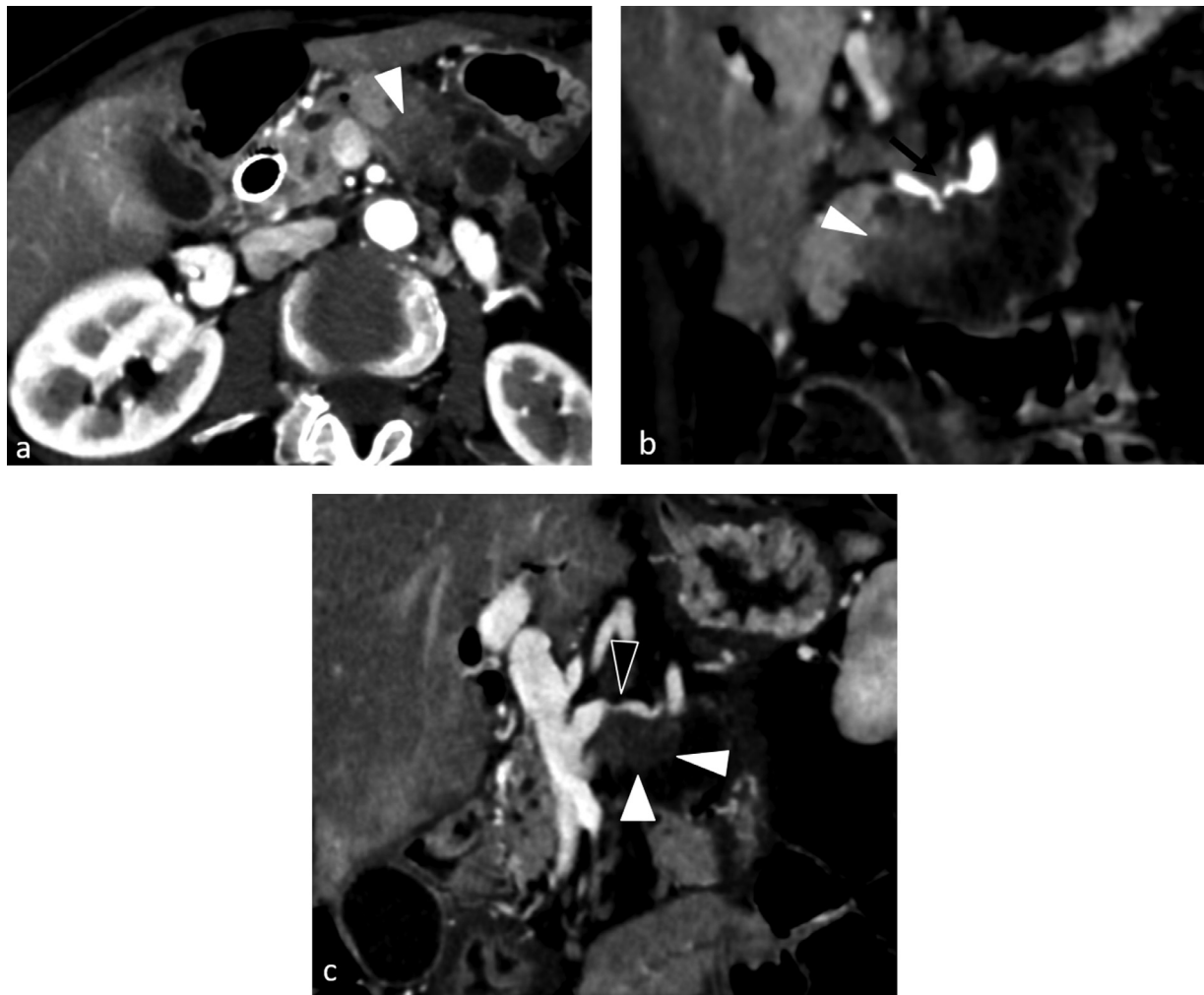


Figure 22 Example of a resectable tumor, computed tomography (CT). Contrast-enhanced CT at the arterial pancreatic phase, (a) axial view and (b and c) coronal maximum intensity projection reconstructions: Tissue lesion in the pancreatic body (white arrowheads) with spread to the splenic artery (black arrow) and a very tight stenosis of the splenic vein (black arrowhead) but no contact with the celiac artery or mesenteric vessels.

Nonresectable Tumors

Locally Advanced Tumors (Figs. 25 and 26)

Arterial

Head/uncinate process:

- Solid tumor contact with the SMA $>180^\circ$
- Solid tumor contact with the CA $>180^\circ$
- Solid tumor contact with the first jejunal SMA branch

Body and tail

- Solid tumor contact with the SMA or CA of $>180^\circ$
- Solid tumor contact with the CA and aortic involvement

VENOUS

Head/uncinate process:

- Unreconstructible SMV/PV due to tumor involvement or occlusion (can be due to tumor or bland thrombus)
- Contact with most proximal draining jejunal branch into the SMV

Body and tail:

- Unreconstructible SMV/PV due to tumor involvement or occlusion (can be due to tumor or bland thrombus)

Metastatic Tumors

- Distant metastasis (including non-regional lymph node metastasis)

Note that vascular invasion does not consistently indicate nonresectability. For instance, invasion of the splenic artery and/or vein does not contraindicate primary surgical resection of a tumor in the left part of the pancreas.

Table 3 recapitulates the resectability criteria depending on the degree of vessel invasion in the NCCN classification.

Pretreatment Imaging Workup

Imaging plays a pivotal role in assessing tumor spread to determine the tumor stage. Ultrasonography contributes little

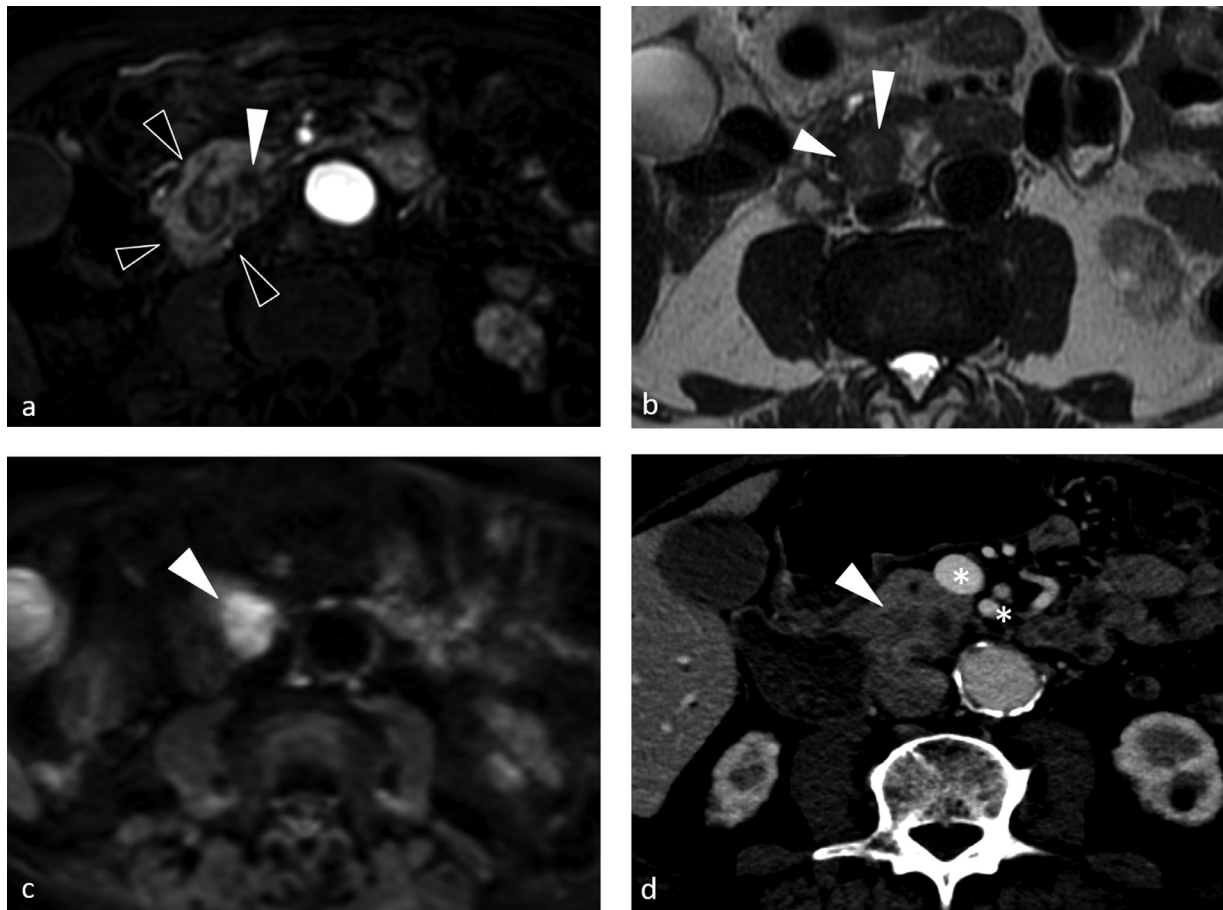


Figure 23 Different example of a resectable tumor, computed tomography (CT), and magnetic resonance imaging (MRI). (a) MRI, postgadolinium T1-weighted fat-suppressed GRE sequence at the arterial pancreatic phase, axial view. (b) MRI, T2 SSFSE sequence, axial view. (c) Diffusion-weighted imaging. (d) Contrast-enhanced CT, portal phase, axial view. Lesion in the posterior pancreatic head (white arrowheads), at a distance from the superior mesenteric artery and vein (asterisks). Note the annular pancreas (black arrowheads).

to staging, whereas CT and MRI are indispensable and complementary. CT is most effective for assessing locoregional spread and MRI for detecting remote metastases. EUS and FDG-PET-CT may be used also but are not performed routinely.

Vascular Spread

Vascular spread governs tumor resectability and must therefore be evaluated in detail. Many studies have compared the diagnostic performance of CT and MRI for predicting vascular invasion and evaluating tumor resectability. In most of the recent studies of CT performance in predicting vascular spread, sensitivity ranged from 70% to 96% and specificity from 82% to 100%.^{28,94-97} Importantly, 2 meta-analyses by Asian groups found fairly low false-positive rates,^{98,99} indicating a low risk of depriving patients of potentially curative surgery. MRI had 70%-80% sensitivity and 96%-99% specificity. Overall performance was similar for CT and MRI in most of the recent studies.^{97,100,101} Nonetheless, CT remains the reference standard for detecting vascular spread, due both to its better spatial resolution, which may translate into higher sensitivity,¹⁰² and to its better reproducibility.

Thus, the diagnostic performance of CT for detecting vascular involvement is very good overall¹⁰³ provided the investigation is performed before any invasive procedures (diagnostic fine needle biopsy or endoscopic drainage) and before starting chemotherapy and/or radiotherapy.

Venous Involvement

Venous involvement typically involves 3 phases: Direct spread, stenosis, and occlusion. Endoluminal invasion of the vessel in contact with the tumor is rare and far more suggestive of pancreatic NET than of pancreatic adenocarcinoma (Fig. 27).

Venous involvement produces direct and indirect signs, as listed below (Fig. 27):

Direct signs

- Occlusion or thrombosis
- Vein contour irregularity/stenosis
- Teardrop deformity of the vein in contact with the tumor

Contact over less than 180° of the vessel circumference with no change in vessel diameter is not highly specific of vascular invasion. A very short stenosis is far more specific.

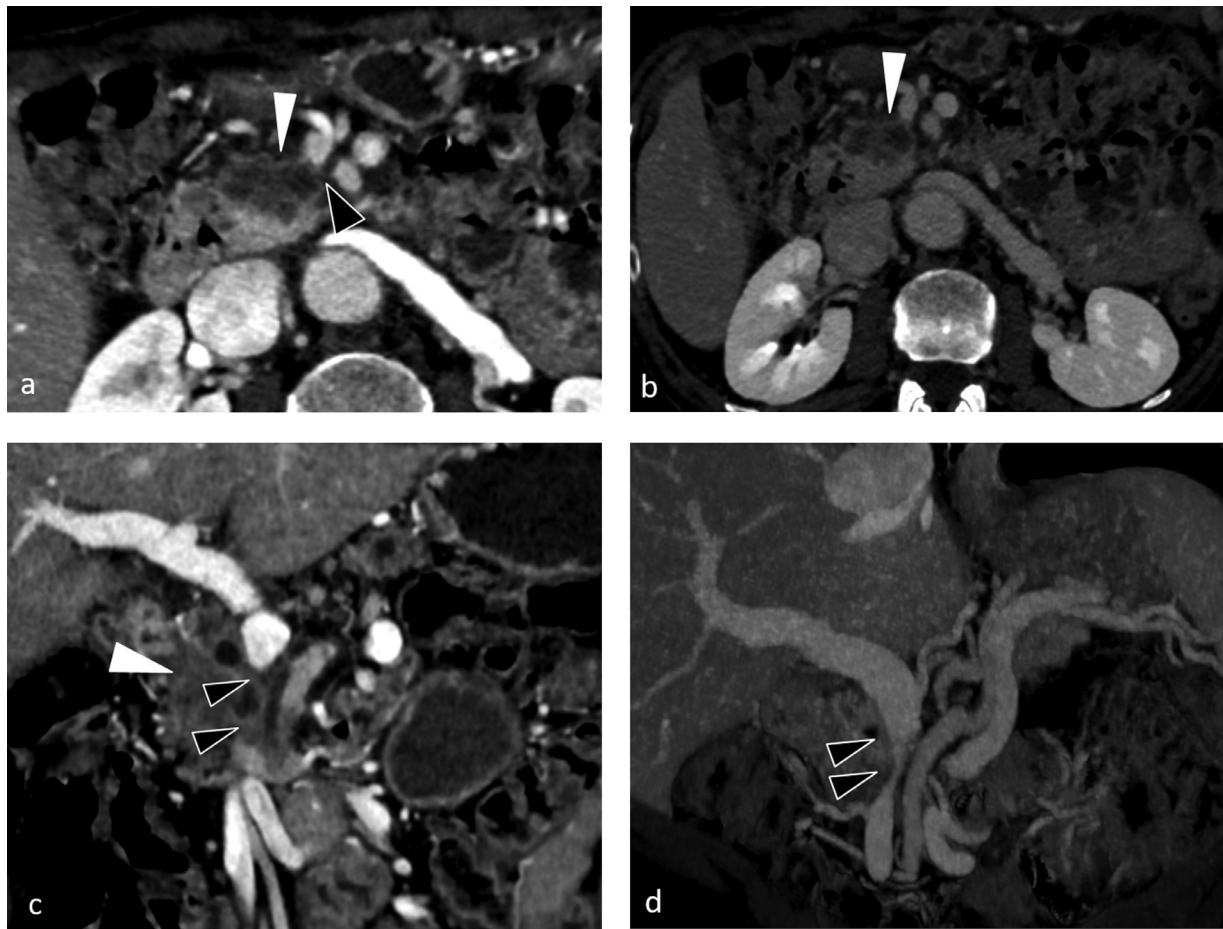


Figure 24 Tumor classified as borderline-resectable in the NCCN classification, computed tomography (CT). Contrast-enhanced CT, axial views at the (a) arterial pancreatic and (b) portal phases; (c) coronal view at the arterial pancreatic phase; and (d) coronal maximum intensity projection reconstruction of a contrast-enhanced acquisition at the portal phase. Lesion in the head of the pancreas (white arrowheads) with encasement of the superior mesenteric vein causing nonocclusive stenosis (black arrowheads) over about 2 cm.

Indirect signs

Venous invasion can produce indirect signs. Thus, involvement of the splenic vein or superior mesenteric vein causes segmental portal hypertension with the development of collaterals about the stomach (from the gastroepiploic vein) or pancreas (from the pancreaticoduodenal arcades). In addition, the spleen may become enlarged if the splenic vein is involved.

Arterial Involvement

Encasement of an artery over more than 180° of its circumference is specific of arterial invasion (Fig. 28).

The Retroportal Space

The retroportal space is a predominant pathway for the dissemination of pancreatic head tumors, notably those located posteriorly. A routine imaging study assessment is indispensable, as invasion of the retroportal space indicates a T3 or, in many cases, a T4 tumor that is not amenable to primary resection.

The retroportal space contains fat tissue that contains the nerve plexus between the uncinate process and

superior mesenteric artery, the superior and inferior pancreaticoduodenal arteries and veins, and lymphatic structures. The retroportal space is bounded laterally by the uncinate process, medially by the superior mesenteric artery, anteriorly by the mesentericoportal vein, posteriorly by the abdominal aorta, superiorly by the right celiac node, and inferiorly by the third duodenum.¹⁰⁴

By CT imaging, invasion is seen as hypoattenuating tissue within the retroportal space that is contiguous with and isoattenuating to the pancreatic tumor.

Lymph Node Invasion

Node status in patients with resectable pancreatic cancer is closely associated with survival.¹⁰⁵ The contribution of both CT and MRI to the diagnosis of node involvement is limited. Although sensitivity has been considerably improved by the introduction of multislice CT and DWI, specificity remains low. CT has only 14% sensitivity.¹⁰⁶ The CT criterion used to diagnose node involvement is a short axis diameter greater than 10 mm. However, many involved nodes are below this cutoff. On the other hand,

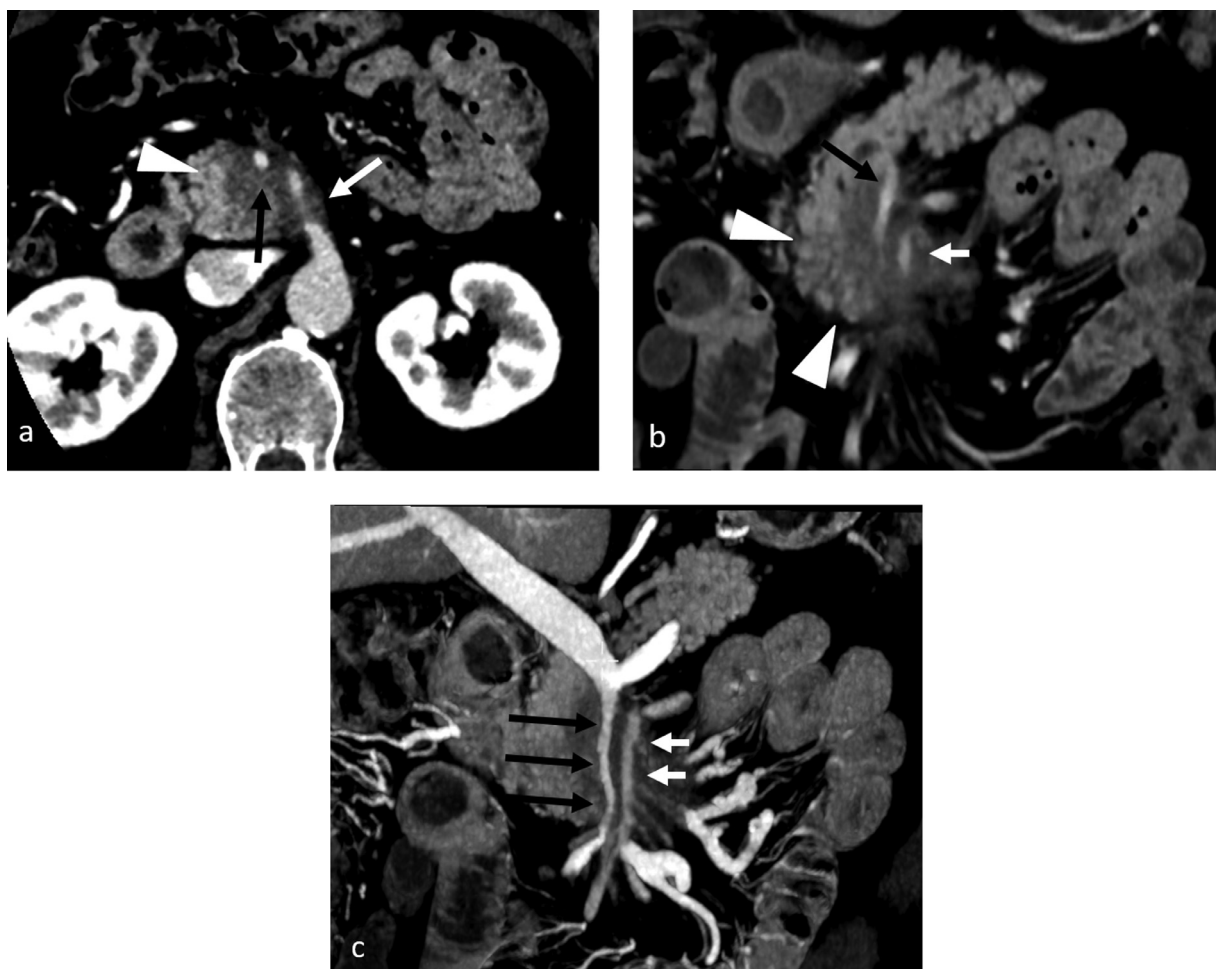


Figure 25 Locally advanced tumor, computed tomography (CT). Contrast-enhanced CT at the arterial pancreatic phase, (a) axial view, (b) coronal view, and (c) coronal maximum intensity projection reconstruction (MIP): Hypoattenuating lesion in the head of the pancreas (white arrowheads) with circumferential encasement of the superior mesenteric vein (black arrowheads) producing an irregular area of stenosis, with involvement of the jejunal veins and 360° encasement of the superior mesenteric artery (white arrows).

inflammatory nodes may measure more than 10 mm. MRI is not superior over CT.

In practice, the presence on CT images of a peripancreatic node with a short axis greater than 10 mm should not influence the treatment strategy for tumors classified as resectable.¹⁰⁷ Involvement of remote nodes (hepatic hilum, root of the mesentery, retroperitoneal space, or aorta-vena cava interval), in contrast, indicates a poor prognosis and classifies the tumor as nonresectable.

PET-CT may be helpful when the diagnosis is in doubt, although its poor spatial resolution results in low sensitivity.¹⁰⁸

EUS has the same limitations as noninvasive imaging modalities, with only fair sensitivity and specificity, but may nevertheless be the best means of evaluating the peripancreatic nodes. Criteria for node involvement are a short axis greater than 5 mm, sharp margins, a rounded shape, and low echogenicity. EUS has a mean accuracy of about 70% for predicting node involvement, whereas specificity is only about 50%.¹⁰⁹

Perineural or Duodenal Spread

A recent study by Chang et al. drew attention to the little known association between CT evidence of extra-pancreatic perineural or duodenal spread and decreased survival after pancreaticoduodenectomy for cephalic pancreatic adenocarcinoma.¹¹⁰ The malignant cells can spread along the fat that extends directly away from the tumor, along the following perineural pathways:

- The plexus pancreaticus capitalis 1, which can be involved by tumors in the superior or middle part of the uncinate process;
- The plexus pancreaticus capitalis 2, at risk for involvement by tumors in the caudal part of the uncinate process;
- The anterior pathway along the gastroduodenal artery plexus and common hepatic artery plexus, potentially involved by tumors in the anterior part of the pancreatic head or isthmus; and

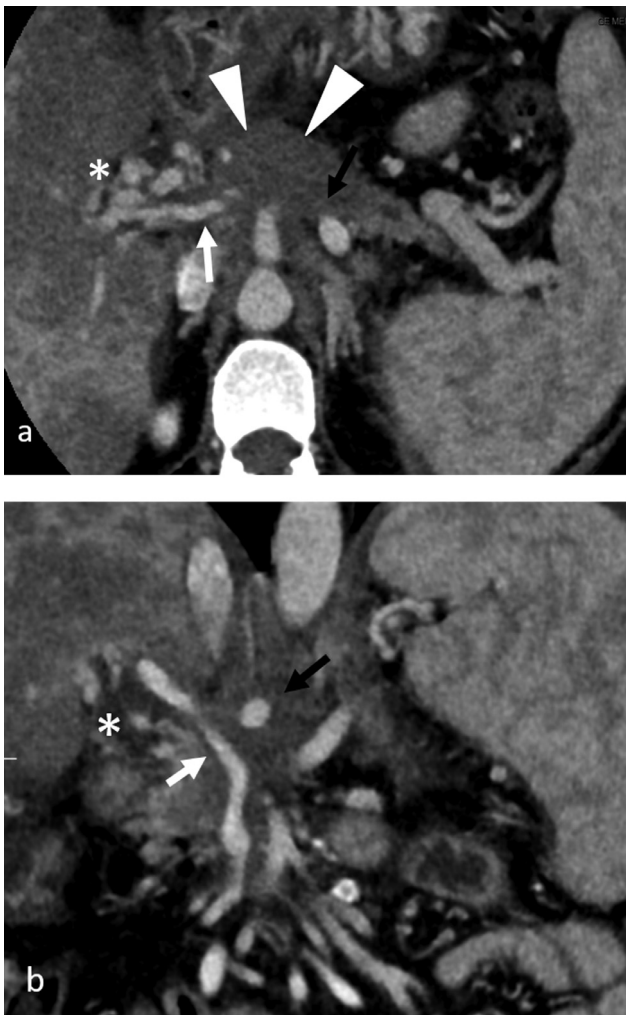


Figure 26 Different example of locally advanced tumor, computed tomography (CT). Contrast-enhanced CT at the arterial pancreatic phase, (a) axial view and (b) coronal view: hypoattenuating infiltrating mass in the isthmus (white arrowhead) with circumferential encasement of the portal vein and superior mesenteric vein (white arrow) responsible for a very tight stenosis with a portal cavernoma (asterisk); note also the circumferential encasement of the celiac artery (black arrow).

- The root of mesentery pathway, which can be invaded by tumors of the uncinate process that extend along the mesenteric perineural plexuses, following the superior mesenteric artery or transverse mesocolon.

Duodenal invasion was defined as CT evidence of hypoattenuating involvement of the duodenal wall extending directly from the pancreatic tumor.¹¹¹ Invasion was defined both as interruption of the normal duodenal wall enhancement by tissue exhibiting the same attenuation as the adjacent pancreatic tumor and by diffuse or nodular thickening of the duodenal wall (Fig. 29).

Metastatic Tumor Spread

About 53% of patients have remote metastases at the diagnosis of pancreatic cancer.¹¹² In addition to remote lymph nodes, the most common sites of metastatic dissemination are the liver and peritoneum. Lung and bone metastases are possible but more delayed sites of involvement.

Liver

Liver metastases are difficult to evaluate on imaging studies. Ultrasonography is not recommended, due to low sensitivity. CT has insufficient accuracy and sensitivity for detecting liver micrometastases, with about 85% negative predictive value 85%.³¹ The only 77%-87% accuracy of CT for establishing resectability^{113,114} is the main limitation of CT as a staging tool in pancreatic adenocarcinoma. Liver metastases are usually seen by CT as small, ill-defined, hypoattenuating images.

MRI performs better than CT for detecting and characterizing liver metastases.^{115,116} Excellent contrast resolution is its main advantage. The introduction of DWI has improved the sensitivity of MRI for detecting liver metastases. Compared to CT and PET-CT, MRI with DWI may have better diagnostic performance characteristics, with 80% sensitivity and 96% specificity.¹¹⁷ Compared to CT, MRI may identify 10% more liver metastases, thereby avoiding unnecessary resection surgery in some patients. DWI is also the most sensitive sequence for detecting liver metastases from pancreatic NETs,¹¹⁸ which are usually seen as small, ill-defined lesions with high signal on DWI images, a low ADC value, intermediate signal on T2-weighted images, gradual postgadolinium enhancement and, in some cases, a hypervascular rim (Fig. 30).

In practice, MRI should be performed routinely before surgery for pancreatic adenocarcinoma. Routine MRI is also required before neoadjuvant therapy in patients with CT signs indicating a borderline-resectable or locally advanced nonmetastatic tumor.²⁴

PET-CT has poor spatial resolution and is consequently not superior over CT or MRI. If the available preliminary results are confirmed,⁶¹ PET-MRI might improve the detection of liver metastases by providing both structural images and functional diffusion and metabolic information.

Peritoneum

In published work, peritoneal metastases were often investigated at the same time as liver metastases. As with the liver, the performance of CT for detecting peritoneal metastases is only fair, with low sensitivity, notably at the early stages. MRI with diffusion sequences may provide better detection performance.

Future Prospects

Computational Medical Imaging (Radiomics) and Texture Analysis

Computational medical imaging, also known as radiomics, is a recently introduced and highly promising discipline that

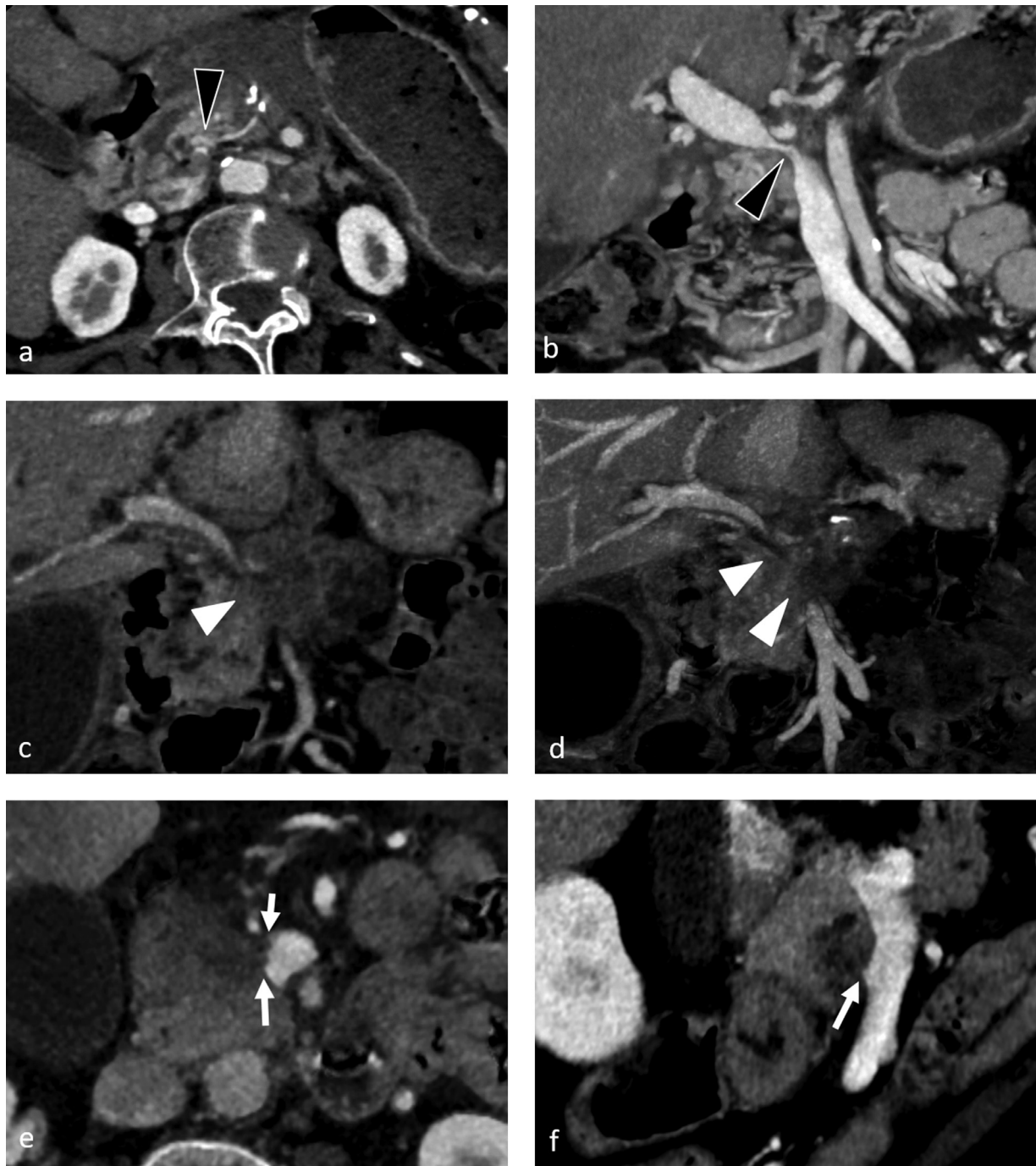


Figure 27 Spread of a primary pancreatic tumor to the veins, computed tomography (CT). Contrast-enhanced CT, portal phase, axial views (a and e), coronal views (c and d) and coronal maximum intensity projection reconstructions (b and f). (a and b) Focal nonocclusive stenosis of the portal vein (black arrowhead). (c and d) Occlusion of the superior mesenteric vein (white arrowheads). (e and f) Tear-drop deformity (white arrows).

consists in using computers to analyze medical images and convert them to complex quantitative data. The high dimensional data thus obtained provide a more detailed characterization of tumor phenotypes. Advantages of computational medical imaging include noninvasiveness, a whole-body assessment, and the ability to monitor the tumor over time

by repeating the test. The ultimate goal is to identify imaging biomarkers that both help to guide medical decisions and provide new insights into cancer biology. Researchers have started to look at the potential contribution of radiomics to the assessment of pancreatic cancer. Associations have been demonstrated between the genomic profile of pancreatic



Figure 28 Spread of a primary pancreatic tumor to the arteries, computed tomography (CT). Contrast-enhanced CT, (a) axial view, (b) coronal view, and (c and d) coronal maximum intensity projection reconstruction. (a and b) Lesion in the head of the pancreas (asterisk) that has spread to the arteries, with circumferential encasement of the superior mesenteric artery (white arrowheads). (c and d) Lesion in the head and isthmus of the pancreas responsible for circumferential encasement of the celiac artery (black arrowheads) and hepatic artery (white arrows), with caliber irregularities.

adenocarcinoma and tumor aggressiveness, treatment response, and clinical outcomes. The most significant genes identified to date are *KRAS*, *CDKN2A*, *TP53*, *SMAD4*, *ATM*, *MLL3*, *BRCA1*, *PDX-1*, *SLC39A4* encoding ZIP4, and *SLC39A4*.¹¹⁹

Another focus of recent research is texture analysis by CT, MRI, or PET-CT. Canellas et al reported that texture analysis and CT features predicted the grade of NETs and might help to predict the risk of recurrence after surgical resection.¹²⁰ Also under study are the differentiation of various stages of fibrosis in AIP and chronic pancreatitis (notably MFCP), malignant architectural disruption in pancreatic adenocarcinoma, and the optimal parameter changes for evaluating the response to chemotherapy and radiotherapy.¹²¹ Texture analysis holds promise but is subject to observer bias, since the images are segmented

manually, and may be influenced by the CT acquisition parameters.¹⁰³ The results are therefore difficult to interpret. Further research is clearly needed before texture analysis can be used in clinical practice.

Artificial Intelligence (AI) – Machine Learning

The use of AI as a medical imaging tool will radically change the clinical practice of radiology over the next few decades. Recent advances have broadened the field of application of AI to medical imaging for computer-assisted tumor detection or diagnosis and for image segmentation, notably at the abdomen.

For the pancreas, fully automated segmentation is available, using a type of artificial neural network known as multi-level deep convolutional networks. Accuracy may be as high

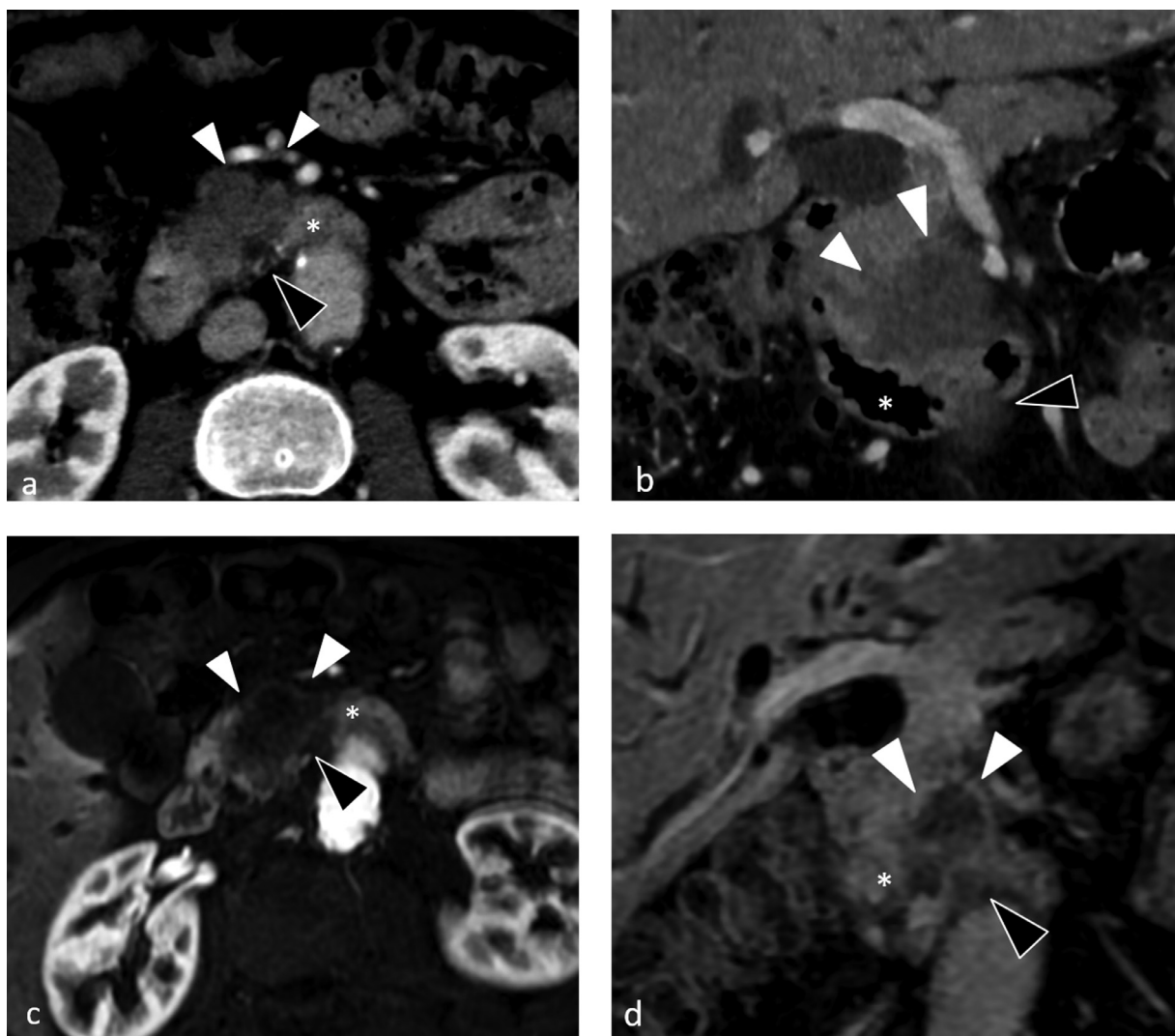


Figure 29 Tumor spread to the duodenum, computed tomography (CT) and magnetic resonance imaging (MRI). (a and b) Contrast-enhanced CT, arterial pancreatic phase, (a) axial view and (b) coronal reconstruction. (c) MRI, T1-weighted fat-suppressed GRE sequence at the arterial phase, axial view. (d) MRI, T1-weighted fat-suppressed GRE sequence at the portal phase, coronal view. Lesion straddling the uncinate process and lower part of the head (white arrows), with posterior extension and spread to the anterior wall of the third part of the duodenum (black arrows: extension; asterisk: duodenum). The stage was T3/N0. R0 margins were obtained during cephalic duodenopancreatectomy performed after neoadjuvant chemotherapy. This patient experienced a local and peritoneal recurrence 6 months after surgery.

as 80%.¹²² The automated detection of node involvement and peritoneal lesions may also hold promise.¹²³

Machine learning can be used to drive additional levels of pancreatic investigations, as well as to characterize various pancreatic disorders (malignancies, inflammatory diseases, fibrous processes, and others). Research is proceeding along these avenues.

Conclusion

The rising incidence of pancreatic cancer is creating a public health issue. Surgical resection with tumor-free margins is the

only potentially curative treatment. Imaging studies therefore play a crucial role, as they allow tumor staging and the identification of patients likely to benefit from surgery. CT is a major tool for assessing locoregional spread, notably to the blood vessels, but performs less well for detecting liver micrometastases and peritoneal metastases. MRI with DWI must therefore be performed before surgery to look for remote metastatic dissemination. Another important contribution of MRI/DWI is the assessment of lesions that are apparently isoattenuating on CT images. The introduction of perfusion modalities and radiomics may benefit the evaluation of pancreatic lesion parameters, thus helping to rule out differentials (notably MFCP). However, these techniques require further investigation and

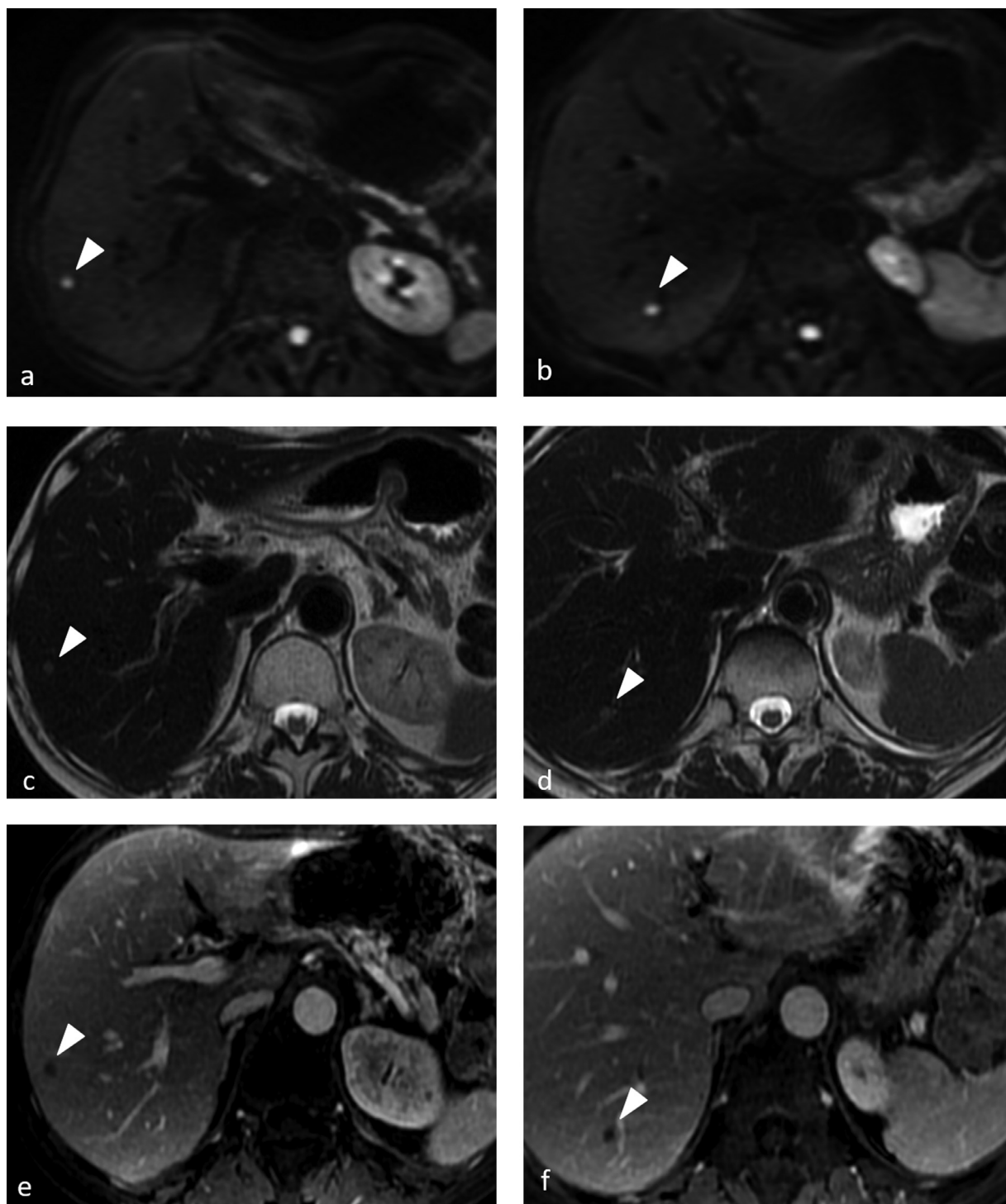


Figure 30 Distal tumor spread: Liver metastases, magnetic resonance imaging (MRI) of the liver. (a and b) Diffusion-weighted imaging, axial views. (c and d) T2 SSFSE sequence, axial view. (e and f) T1-weighted fat-suppressed GRE sequence at the portal phase, axial view. Two lesions, each 1 mm in size, are visible in segment VI (at the top) and segment VII. Both lesions produce high diffusion signal, intermediate T2 signal, and low signal at the portal phase. These lesions were not visible by computed tomography. Thus, by providing the diagnosis of metastatic disease, MRI allowed this patient to avoid unnecessary surgery.

standardization. Finally, neoadjuvant treatment is a recently developed strategy that raises challenges with the imaging study assessment of the tumor response.

References

1. Siegel RL, Miller KD, Jemal A: Cancer statistics, 2017. *CA Cancer J Clin* 67:7-30, 2017

2. Rahib L, Smith BD, Aizenberg R, et al: Projecting cancer incidence and deaths to 2030: The unexpected burden of thyroid, liver, and pancreas cancers in the United States. *Cancer Res* 74:2913-2921, 2014
3. Li D, Xie K, Wolff R, et al: Pancreatic cancer. *Lancet* 363:1049-1057, 2004
4. Hidalgo M: Pancreatic cancer. *N Engl J Med* 362:1605-1617, 2010
5. Seufferlein T, Bachet JB, Van Cutsem E, et al: Pancreatic adenocarcinoma: ESMO-ESDO Clinical Practice Guidelines for diagnosis, treatment and follow-up. *Ann Oncol* 23(suppl 7):vii33-vii40, 2012
6. Wagner M, Redaelli C, Lietz M, et al: Curative resection is the single most important factor determining outcome in patients with pancreatic adenocarcinoma. *Br J Surg* 91:586-594, 2004
7. Ryan DP, Hong TS, Bardeesy N: Pancreatic adenocarcinoma. *N Engl J Med* 371:1039-1049, 2014
8. Kalser MH, Barkin J, MacIntyre JM: Pancreatic cancer. Assessment of prognosis by clinical presentation. *Cancer* 56:397-402, 1985
9. Chari ST, et al: Probability of pancreatic cancer following diabetes: A population-based study. *Gastroenterology* 129:504-511, 2005
10. Huang Z, Liu F: Diagnostic value of serum carbohydrate antigen 19-9 in pancreatic cancer: A meta-analysis. *Tumour Biol J Int Soc Oncodev Biol Med* 35:7459-7465, 2014
11. Ballehaninna UK, Chamberlain RS: The clinical utility of serum CA 19-9 in the diagnosis, prognosis and management of pancreatic adenocarcinoma: An evidence-based appraisal. *J Gastrointest Oncol* 3:15, 2012
12. van Roessel S, Kasumova GG, Verheij J, et al: International validation of the Eighth Edition of the American Joint Committee on Cancer (AJCC) TNM staging system in patients with resected pancreatic cancer. *JAMA Surg* 153:e183617, 2018
13. Cong L, Liu Q, Zhang R, et al: Tumor size classification of the 8th edition of TNM staging system is superior to that of the 7th edition in predicting the survival outcome of pancreatic cancer patients after radical resection and adjuvant chemotherapy. *Sci Rep* 8:10383, 2018
14. Wang L, Lv K, Chang X-Y, et al: Contrast-enhanced ultrasound study of primary hepatic angiosarcoma: a pitfall of non-enhancement. *Eur J Radiol* 81:2054-2059, 2012
15. Conrad C, Fernández-del Castillo C: Preoperative evaluation and management of the pancreatic head mass: Management of Pancreatic Head Mass. *J Surg Oncol* 107:23-32, 2013
16. Karlson B-M, Ekblom A, Lindgren PG, et al: Abdominal US for diagnosis of pancreatic tumor: Prospective cohort analysis. *Radiology* 213:107-111, 1999
17. Maringhini A, Ciambra M, Raimondo M, et al: Clinical presentation and ultrasonography in the diagnosis of pancreatic cancer: *Pancreas* 1993;8:146-50.
18. Lee ES: Imaging diagnosis of pancreatic cancer: A state-of-the-art review. *World J Gastroenterol* 20:7864, 2014
19. Fan Z, Li Y, Yan K, et al: Application of contrast-enhanced ultrasound in the diagnosis of solid pancreatic lesions—A comparison of conventional ultrasound and contrast-enhanced CT. *Eur J Radiol* 82:1385-1390, 2013
20. D'Onofrio M, Biagioli E, Gerardi C, et al: Diagnostic Performance of Contrast-Enhanced Ultrasound (CEUS) and Contrast-Enhanced Endoscopic Ultrasound (ECEUS) for the differentiation of pancreatic lesions: A systematic review and meta-analysis. *Ultraschall Med - Eur J Ultrasound* 35:515-521, 2014
21. Kersting S, Konopke R, Kersting F, et al: Quantitative perfusion analysis of transabdominal contrast-enhanced ultrasonography of pancreatic masses and carcinomas. *Gastroenterology* 137:1903-1911, 2009
22. Kawada N, Tanaka S: Elastography for the pancreas: Current status and future perspective. *World J Gastroenterol* 22:3712, 2016
23. Kawada N, Tanaka S, Uehara H, et al: Feasibility of second-generation transabdominal ultrasound-elastography to evaluate solid pancreatic tumors: Preliminary report of 36 cases. *Pancreas* 41:978-980, 2012
24. Zins M, Matos C, Cassinotto C: Pancreatic adenocarcinoma staging in the era of preoperative chemotherapy and radiation therapy. *Radiology* 287:374-390, 2018
25. Tamm EP, Balachandran A, Bhosale PR, et al: Imaging of pancreatic adenocarcinoma: Update on staging/resectability. *Radiol Clin North Am* 50:407-428, 2012
26. Al-Hawary MM, Francis IR, Chari ST, et al: Pancreatic ductal adenocarcinoma radiology reporting template: Consensus Statement of the Society of Abdominal Radiology and the American Pancreatic Association. *Radiology* 270:248-260, 2014
27. Zins M, Fontanelle L, Lenoir S, et al: Multidetector CT and MRI in pancreatic diseases. *Journal de radiologie* 84:484-496, 2003. discussion 497-8 [Article in French]
28. Zamboni GA, Kruskal JB, Vollmer CM, et al: Pancreatic adenocarcinoma: Value of multidetector CT angiography in preoperative evaluation. *Radiology* 245:770-778, 2007
29. Goshima S, Kanematsu M, Kondo H, et al: Pancreas: Optimal scan delay for contrast-enhanced multi-detector row CT. *Radiology* 241:167-174, 2006
30. Freeny PC, Marks WM, Ryan JA, et al: Pancreatic ductal adenocarcinoma: Diagnosis and staging with dynamic CT. *Radiology* 166:125-133, 1988
31. Valls C, Andia E, Sanchez A, et al: Dual-phase helical CT of pancreatic adenocarcinoma: Assessment of resectability before surgery. *Am J Roentgenol* 178:821-826, 2002
32. Wong JC, Raman S: Surgical resectability of pancreatic adenocarcinoma: CTA. *Abdom Imaging* 35:471-480, 2010
33. Bluemke DA, Cameron JL, Hruban RH, et al: Potentially resectable pancreatic adenocarcinoma: Spiral CT assessment with surgical and pathologic correlation. *Radiology* 197:381-385, 1995
34. Legmann P, Vignaux O, Dousset B, et al: Pancreatic tumors: Comparison of dual-phase helical CT and endoscopic sonography. *Am J Roentgenol* 170:1315-1322, 1998
35. Bronstein YL, Loyer EM, Kaur H, et al: Detection of small pancreatic tumors with multiphase helical CT. *Am J Roentgenol* 182:619-623, 2004
36. Macari M, Spieler B, Kim D, et al: Dual-source dual-energy MDCT of pancreatic adenocarcinoma: Initial observations with data generated at 80 kVp and at simulated weighted-average 120 kVp. *Am J Roentgenol* 194:W27-W32, 2010
37. Patel BN, Thomas JV, Lockhart ME, et al: Single-source dual-energy spectral multidetector CT of pancreatic adenocarcinoma: Optimization of energy level viewing significantly increases lesion contrast. *Clin Radiol* 68:148-154, 2013
38. Brook OR, Gourtsoyianni S, Brook A, et al: Split-bolus spectral multidetector CT of the pancreas: Assessment of radiation dose and tumor conspicuity. *Radiology* 269:139-148, 2013
39. Bhosale P, Le O, Balachandran A, et al: Quantitative and qualitative comparison of single-source dual-energy computed tomography and 120-kVp computed tomography for the assessment of pancreatic ductal adenocarcinoma. *J Comput Assist Tomogr* 39:907-913, 2015
40. Kim JK, Ha HK, Han DJ, et al: CT analysis of postoperative tumor recurrence patterns in periampullary cancer. *Abdom Imaging* 28:384-391, 2003
41. Prokesch RW, Chow LC, Beaulieu CF, et al: Isoattenuating pancreatic adenocarcinoma at multidetector row CT: Secondary signs. *Radiology* 224:764-768, 2002
42. Ishigami K, Yoshimitsu K, Irie H, et al: Diagnostic value of the delayed phase image for iso-attenuating pancreatic carcinomas in the pancreatic parenchymal phase on multidetector computed tomography. *Eur J Radiol* 69:139-146, 2009
43. Yoon SH, Lee JM, Cho JY, et al: Small (≤ 20 mm) pancreatic adenocarcinomas: analysis of enhancement patterns and secondary signs with multiphase multidetector CT. *Gastrointest Imaging* 259:11, 2011
44. Morana G: Staging cancer of the pancreas. *Cancer Imaging* 10:S137-S141, 2010
45. Kim JH, Park SH, Yu ES, et al: Visually isoattenuating pancreatic adenocarcinoma at dynamic-enhanced CT: Frequency, clinical and pathologic characteristics, and diagnosis at imaging examinations. *Radiology* 257:87-96, 2010
46. Legrand L, Duchatelle V, Molinié V, et al: Pancreatic adenocarcinoma: MRI conspicuity and pathologic correlations. *Abdom Imaging* 40:85-94, 2015
47. Ichikawa T, Erturk SM, Motosugi U, et al: High-b value diffusion-weighted MRI for detecting pancreatic adenocarcinoma: Preliminary results. *Am J Roentgenol* 188:409-414, 2007
48. Fukukura Y, Takumi K, Kamimura K, et al: Pancreatic adenocarcinoma: Variability of diffusion-weighted MR imaging findings. *Radiology* 263:732-740, 2012

49. Kartalis N, Lindholm TL, Aspelin P, et al: Diffusion-weighted magnetic resonance imaging of pancreas tumours. *Eur Radiol* 19:1981-1990, 2009
50. Barral M, Taouli B, Guiu B, et al: Diffusion-weighted MR imaging of the pancreas: Current status and recommendations. *Radiology* 274:45-63, 2015
51. Hayano K, Miura F, Amano H, et al: Correlation of apparent diffusion coefficient measured by diffusion-weighted MRI and clinicopathologic features in pancreatic cancer patients. *J Hepato-Biliary-Pancreat Sci* 20:243-248, 2013
52. Garcés-Descovich A, Morrison TC, Beker K, et al: DWI of pancreatic ductal adenocarcinoma: A pilot study to estimate the correlation with metastatic disease potential and overall survival. *Am J Roentgenol* 212:323-331, 2019
53. Okada K, Hirono S, Kawai M, et al: Value of apparent diffusion coefficient prior to neoadjuvant therapy is a predictor of histologic response in patients with borderline resectable pancreatic carcinoma. *J Hepato-Biliary-Pancreat Sci* 24:161-168, 2017
54. Fukukura Y, Shindo T, Hakamada H, et al: Diffusion-weighted MR imaging of the pancreas: optimizing b-value for visualization of pancreatic adenocarcinoma. *Eur Radiol* 26:3419-3427, 2016
55. Bournet B, Souque A, Senesse P, et al: Endoscopic ultrasound-guided fine-needle aspiration biopsy coupled with KRAS mutation assay to distinguish pancreatic cancer from pseudotumoral chronic pancreatitis. *Endoscopy* 41:552-557, 2009
56. Iglesias-Garcia J, Poley J-W, Larghi A, et al: Feasibility and yield of a new EUS histology needle: results from a multicenter, pooled, cohort study. *Gastrointest Endosc* 73:1189-1196, 2011
57. Hewitt MJ, McPhail MJW, Possamai L, et al: EUS-guided FNA for diagnosis of solid pancreatic neoplasms: A meta-analysis. *Gastrointest Endosc* 75:319-331, 2012
58. Fritscher-Ravens A., Topalidis T. Comparison of endoscopic ultrasound-guided fine needle aspiration for focal pancreatic lesions in patients with normal parenchyma and chronic pancreatitis. 2002;97:8.
59. Jha P, Bijan B: PET/CT for pancreatic malignancy: Potential and pitfalls. *J Nucl Med Technol* 43:92-97, 2015
60. Sahani DV, Bonaffini PA, Catalano OA, et al: State-of-the-art PET/CT of the pancreas: Current role and emerging indications. *Radio Graphics* 32:1133-1158, 2012
61. Joo I, Lee JM, Lee DH, et al: Preoperative assessment of pancreatic cancer with FDG PET/MR imaging versus FDG PET/CT plus contrast-enhanced multidetector CT: A prospective preliminary study. *Radiology* 282:149-159, 2017
62. Yamada Y, Mori H, Matsumoto S, et al: Pancreatic adenocarcinoma versus chronic pancreatitis: Differentiation with triple-phase helical CT. *Abdom Imaging* 35:163-171, 2010
63. Frampas E, Morla O, Regenet N, et al: Masse solide du pancréas: tumeur ou inflammation? *J Radiol Diagn Interv* 94:751-766, 2013
64. Yadav AK, Sharma R, Kandasamy D, et al: Perfusion CT – Can it resolve the pancreatic carcinoma versus mass forming chronic pancreatitis conundrum? *Pancreatol* 16:979-987, 2016
65. Dietrich CF, Ignee A, Braden B, et al: Improved differentiation of pancreatic tumors using contrast-enhanced endoscopic ultrasound. *Clin Gastroenterol Hepatol* 6:590-597.e1, 2008
66. Matsubara H, Itoh A, Kawashima H, et al: Dynamic quantitative evaluation of contrast-enhanced endoscopic ultrasonography in the diagnosis of pancreatic diseases. *Pancreas* 40:1073-1079, 2011
67. Faccioli N, Crippa S, Bassi C, et al: Contrast-enhanced ultrasonography of the pancreas. *Pancreatol* 9:560-566, 2009
68. Ma X, Zhao X, Ouyang H, et al: Quantified ADC histogram analysis: A new method for differentiating mass-forming focal pancreatitis from pancreatic cancer. *Acta Radiol Stockh Swed* 55:785-792, 2014
69. Shimosegawa T, Chari ST, Frulloni L, et al: International consensus diagnostic criteria for autoimmune pancreatitis: Guidelines of the International Association of Pancreatology. *Pancreas* 40:352-358, 2011
70. Manfredi R, Graziani R, Cicero C, et al: Autoimmune pancreatitis: CT patterns and their changes after steroid treatment. *Radiology* 247:435-443, 2008
71. Chari ST: Diagnosis of autoimmune pancreatitis using its five cardinal features: Introducing the Mayo Clinic's HISORt criteria. *J Gastroenterol* 42(Suppl 18):39-41, 2007
72. Rebours V, Lévy P: The two types of auto-immune pancreatitis. *Presse Med* 41:580-592, 2012. [Article in French]
73. Negrelli R, Manfredi R, Pedrinolla B, et al: Pancreatic duct abnormalities in focal autoimmune pancreatitis: MR/MRCP imaging findings. *Eur Radiol* 25:359-367, 2015
74. Muhi A, Ichikawa T, Motosugi U, et al: Mass-forming autoimmune pancreatitis and pancreatic carcinoma: Differential diagnosis on the basis of computed tomography and magnetic resonance cholangiopancreatography, and diffusion-weighted imaging findings. *J Magn Reson Imaging JMIR* 35:827-836, 2012
75. Sugiyama Y, Fujinaga Y, Kadoya M, et al: Characteristic magnetic resonance features of focal autoimmune pancreatitis useful for differentiation from pancreatic cancer. *Jpn J Radiol* 30:296-309, 2012
76. Kim HJ, Kim YK, Jeong WK, et al: Pancreatic duct “icicle sign” on MRI for distinguishing autoimmune pancreatitis from pancreatic ductal adenocarcinoma in the proximal pancreas. *Eur Radiol* 25:1551-1560, 2015
77. Lee S, Kim JH, Kim SY, et al: Comparison of diagnostic performance between CT and MRI in differentiating non-diffuse-type autoimmune pancreatitis from pancreatic ductal adenocarcinoma. *Eur Radiol* 28:5267-5274, 2018
78. Sugumar A, Chari ST: Distinguishing pancreatic cancer from autoimmune pancreatitis: A comparison of two strategies. *Clin Gastroenterol Hepatol* 7:S59-S62, 2009
79. Blasbalg R, Baroni RH, Costa DN, et al: MRI features of groove pancreatitis. *AJR Am J Roentgenol* 189:73-80, 2007
80. Ren S, Chen X, Wang Z, et al: Differentiation of hypovascular pancreatic neuroendocrine tumors from pancreatic ductal adenocarcinoma using contrast-enhanced computed tomography. *PLoS One* 14, 2019. [cited 2019 May 4]. Available from: <https://www.ncbi.nlm.nih.gov/pmc/articles/PMC6358067/>
81. Brenner R, Metens T, Bali M, et al: Pancreatic neuroendocrine tumor: Added value of fusion of T2-weighted imaging and high b-value diffusion-weighted imaging for tumor detection. *Eur J Radiol* 81:e746-e749, 2012
82. Lotfalizadeh E, Ronot M, Wagner M, et al: Prediction of pancreatic neuroendocrine tumour grade with MR imaging features: Added value of diffusion-weighted imaging. *Eur Radiol* 27:1748-1759, 2017
83. Dromain C, Déandréis D, Scoazec J-Y, et al: Imaging of neuroendocrine tumors of the pancreas. *Diagn Interv Imaging* 97:1241-1257, 2016
84. Moussa A, Mitry E, Hammel P, et al: Pancreatic metastases: A multicentric study of 22 patients. *Gastroenterol Clin Biol* 28:872-876, 2004
85. Boudghène FP, Deslandes PM, LeBlanche AF, et al: US and CT imaging features of intrapancreatic metastases. *J Comput Assist Tomogr* 18:905-910, 1994
86. Low G, Panu A, Millo N, et al: Multimodality imaging of neoplastic and nonneoplastic solid lesions of the pancreas. *Radiogr Rev Publ Radiol Soc N Am Inc* 31:993-1015, 2011
87. Jorret D, Soyer P, Terris B, et al: MR imaging features of pancreatic acinar cell carcinoma. *Diagn Interv Imaging* 100:427-435, 2019
88. Nishimura M, Wada H, Eguchi H, et al: [A case report of acinar cell carcinoma of pancreas with extensive intraductal growth to the branch - Main pancreatic duct]. *Gan To Kagaku Ryoho* 44:1568-1570, 2017
89. Tempero MA, Malafa MP, Al-Hawary M, et al: Pancreatic adenocarcinoma, Version 2.2017, NCCN clinical practice guidelines in oncology. *J Natl Compr Cancer Netw JNCCN* 15:1028-1061, 2017
90. Gillen S, Schuster T, Meyer Zum Büschenfelde C, et al: Preoperative/neoadjuvant therapy in pancreatic cancer: A systematic review and meta-analysis of response and resection percentages. *PLoS Med* 7: e1000267, 2010
91. Neuzillet C, Gaujoux S, Williet N, et al: Pancreatic cancer: French clinical practice guidelines for diagnosis, treatment and follow-up (SNFGE, FFCU, GERCOR, UNICANCER, SFCD, SFED, SFRO, ACHBT, AFC). *Dig Liver Dis* 50:1257-1271, 2018
92. Khorana AA, Mangu PB, Berlin J, et al: Potentially curable pancreatic cancer: American Society of Clinical Oncology Clinical Practice Guideline Update. *J Clin Oncol* 35:2324-2328, 2017
93. Varadhachary GR, Tamm EP, Abbruzzese JL, et al: Borderline resectable pancreatic cancer: Definitions, management, and role of preoperative therapy. *Ann Surg Oncol* 13:1035-1046, 2006

94. Fletcher JG, Wiersema MJ, Farrell MA, et al: Pancreatic malignancy: Value of arterial, pancreatic, and hepatic phase imaging with multi-detector row CT. *Radiology* 229:81-90, 2003
95. Catalano C, Laghi A, Fraioli F, et al: Pancreatic carcinoma: The role of high-resolution multislice spiral CT in the diagnosis and assessment of resectability. *Eur Radiol* 13:149-156, 2003
96. Karmazanovsky G, Fedorov V, Kubyshev V, et al: Pancreatic head cancer: Accuracy of CT in determination of resectability. *Abdom Imaging* 30:488-500, 2005
97. Koelblinger C, Ba-Ssalamah A, Goetzinger P, et al: Gadobenate dimeglumine-enhanced 3.0-T MR imaging versus multiphase 64-detector row CT: Prospective evaluation in patients suspected of having pancreatic cancer. *Radiology* 259:757-766, 2011
98. Zhao W-Y, Luo M, Sun Y-W, et al: Computed tomography in diagnosing vascular invasion in pancreatic and periampullary cancers: A systematic review and meta-analysis. *Hepatobiliary Pancreat Dis Int* 8:457-464, 2009
99. Yang R, Lu M, Qian X, et al: Diagnostic accuracy of EUS and CT of vascular invasion in pancreatic cancer: A systematic review. *J Cancer Res Clin Oncol* 140:2077-2086, 2014
100. Park HS, Lee JM, Choi HK, et al: Preoperative evaluation of pancreatic cancer: Comparison of gadolinium-enhanced dynamic MRI with MR cholangiopancreatography versus MDCT. *J Magn Reson Imaging JMRI* 30:586-595, 2009
101. Chen F-M, Ni J-M, Zhang Z-Y, et al: Presurgical evaluation of pancreatic cancer: A comprehensive imaging comparison of CT versus MRI. *AJR Am J Roentgenol* 206:526-535, 2016
102. Nishiharu T, Yamashita Y, Abe Y, et al: Local extension of pancreatic carcinoma: Assessment with thin-section helical CT versus with breath-hold fast MR imaging—ROC analysis. *Radiology* 212:445-452, 1999
103. Somers I, Bipat S. Contrast-enhanced CT in determining resectability in patients with pancreatic carcinoma: a meta-analysis of the positive predictive values of CT. - PubMed - NCBI [Internet]. [cited 2019 May 4]. Available from: <https://www.ncbi.nlm.nih.gov/pubmed/28093626>.
104. Gockel I, Domeyer M, Wolloscheck T, et al: Resection of the mesopancreas (RMP): A new surgical classification of a known anatomical space. *World J Surg Oncol* 5:44, 2007
105. Tol JAMG, Gouma DJ, Bassi C, et al: Definition of a standard lymphadenectomy in surgery for pancreatic ductal adenocarcinoma: A consensus statement by the International Study Group on Pancreatic Surgery (ISGPS). *Surgery* 156:591-600, 2014
106. Roche CJ, Hughes ML, Garvey CJ, et al: CT and pathologic assessment of prospective nodal staging in patients with ductal adenocarcinoma of the head of the pancreas. *AJR Am J Roentgenol* 180:475-480, 2003
107. Moutardier V, Giovannini M, Magnin V, et al: [How to improve treatment of resectable pancreatic adenocarcinomas? Surgical resection, histopathological examination, adjuvant therapies]. *Gastroenterol Clin Biol* 28:1083-1091, 2004
108. Buchs NC, Chilcott M, Poletti P-A, et al: Vascular invasion in pancreatic cancer: Imaging modalities, preoperative diagnosis and surgical management. *World J Gastroenterol WJG* 16:818-831, 2010
109. Tio TL, Tytgat GN, Cikota RJ, et al: Ampullopapillary carcinoma: Preoperative TNM classification with endosonography. *Radiology* 175:455-461, 1990
110. Chang ST, Jeffrey RB, Patel BN, et al: Preoperative multidetector CT diagnosis of extrapancreatic perineural or duodenal invasion is associated with reduced postoperative survival after pancreaticoduodenectomy for pancreatic adenocarcinoma: Preliminary experience and implications for patient care. *Radiology* 281:816-825, 2016
111. Padilla-Thornton AE, Willmann JK, Jeffrey RB: Adenocarcinoma of the uncinate process of the pancreas: MDCT patterns of local invasion and clinical features at presentation. *Eur Radiol* 22:1067-1074, 2012
112. Al-Hawary MM, Kaza RK, Wasnik AP, et al: Staging of pancreatic cancer: Role of imaging. *Semin Roentgenol* 48:245-252, 2013
113. Vargas R, Nino-Murcia M, Trueblood W, et al: MDCT in pancreatic adenocarcinoma: Prediction of vascular invasion and resectability using a multiphase technique with curved planar reformations. *AJR Am J Roentgenol* 182:419-425, 2004
114. Manak E, Merkel S, Klein P, et al: Resectability of pancreatic adenocarcinoma: assessment using multidetector-row computed tomography with multiplanar reformations. *Abdom Imaging* 34:75-80, 2009
115. Jeon SK, Lee JM, Joo I, et al: Magnetic resonance with diffusion-weighted imaging improves assessment of focal liver lesions in patients with potentially resectable pancreatic cancer on CT. *Eur Radiol* 28:3484-3493, 2018
116. Motosugi U, Ichikawa T, Morisaka H, et al: Detection of pancreatic carcinoma and liver metastases with gadoteric acid-enhanced MR imaging: Comparison with contrast-enhanced multi-detector row CT. *Radiology* 260:446-453, 2011
117. Marion-Audibert AM, Vullierme MP, Ronot M, et al: Routine MRI with DW sequences to detect liver metastases in patients with potentially resectable ductal carcinoma and normal liver CT: A prospective multicenter study. *AJR Am J Roentgenol* 211:W217-W225, 2018
118. d'Assignies G, Fina P, Bruno O, et al: High sensitivity of diffusion-weighted MR imaging for the detection of liver metastases from neuroendocrine tumors: Comparison with T2-weighted and dynamic gadolinium-enhanced MR imaging. *Radiology* 268:390-399, 2013
119. Bramswig NC, Kaestner KH: Organogenesis and functional genomics of the endocrine pancreas. *Cell Mol Life Sci CMLS* 69:2109-2123, 2012
120. Canellas R, Burk KS, Parakh A, et al: Prediction of pancreatic neuroendocrine tumor grade based on CT features and texture analysis. *AJR Am J Roentgenol* 210:341-346, 2018
121. Almeida RR, Lo GC, Patino M, et al: Advances in pancreatic CT imaging. *Am J Roentgenol* 211:52-66, 2018
122. Roth HR, Lu L, Farag A, et al: DeepOrgan: Multi-level deep convolutional networks for automated pancreas segmentation. *ArXiv150606448 Cs* [Internet]. 2015. [cited 2019 May 5]; Available from: <http://arxiv.org/abs/1506.06448>
123. Summers RM: Progress in fully automated abdominal CT interpretation. *AJR Am J Roentgenol* 207:67-79, 2016